CERTS MICROGRID
LABORATORY TEST BED

Microgrid Fault Protection Based on Symmetrical and Differential Current Components

APPENDIX P

Prepared For:
California Energy Commission
Public Interest Energy Research Program

Prepared By:
Lawrence Berkeley National Laboratory

CERTS
CONSORTIUM FOR ELECTRIC RELIABILITY TECHNOLOGY SOLUTIONS

Prepared By:
Lawrence Berkeley National Laboratory
Joseph H. Eto, Principal Investigator
Berkeley, CA 94720
Hassan Nikkhajoei and Robert H. Lasseter, University of Wisconsin
Nancy J. Lewis, Lawrence Berkeley National Laboratory
Commission Contract No. 500-03-024
LBNL-802E

Prepared For:
Public Interest Energy Research (PIER)
California Energy Commission

Bernard Treanton
Contract Manager

Mike Gravely
Program Area Lead
ENERGY SYSTEMS INTEGRATION

Mike Gravely
Office Manager
ENERGY SYSTEMS RESEARCH

Martha Krebs, Ph.D.
PIER Director

Thom Kelly, Ph.D.
Deputy Director
ENERGY RESEARCH & DEVELOPMENT DIVISION

Melissa Jones
Executive Director

Microgrid Fault Protection Based on Symmetrical and Differential Current Components

Prepared by

Hassan Nikkhajoei and Robert H. Lasseter

Wisconsin Power Electronics Research Center
Department of Electrical and Computer Engineering
University of Wisconsin-Madison

December 2006

Table of Contents

Index of Figures

1. Introduction

The objective of this study is to develop a systematic approach for protecting a microgrid, in particular the AEP microgrid, against Single Line-to-Ground (SLG) and Line-to-Line (LL) faults. A microgrid is a part of a large power system in which a number of sources, usually attached to a power electronic converter, and loads are clustered so that the microgrid can operate independent of the main power system [1], [2]. In general, a microgrid can operate in both the grid-connected mode and the islanded mode where the microgrid is disconnected from the main power system by a fast semiconductor switch called static switch, Fig. 1.

It is essential to protect a microgrid in both the grid-connected and the islanded modes of operation against for all SLG and LL faults. The philosophy of protection is to disconnect the static switch for all classes of faults. With the static switch open (islanded mode), output currents of the microgrid sources are limited by the corresponding power electronic converter to 2.0 pu. Therefore, a microgrid cannot be protected against faults based on traditional over-current protection since there is not adequate fault currents in the islanded mode of operation.

The main challenge for protecting a microgrid arises from the fact that power can flow in both directions in each feeder of a microgrid. Close to each local load, there may exist two or more sources that contribute to the load power, Fig. 1. The sources can be located in both sides of the load and therefore, power flows in opposite directions from the two sources towards the load. As a results, in a section of the feeder, e.g. Zone 3 of Fig. 1, that is between the source A_1 and the load, power flows in one direction and in the other section, i.e. Zone 4, power flows in an opposite direction. It is to be noted that, in conventional distribution systems, power always flows in one direction, from the distribution substation towards the loads.

It was initially thought that a microgrid can be protected, at least for SLG faults, based on differential components of phase currents. However, studies showed that each relay, which corresponds to a microgrid protection zone, e.g. the Relay 4 of Fig. 1, can only detect SLG faults that occur in the up-stream zone of the relay, i.e. Zone 4 of Fig. 1. The relays do not detect an SLG fault in a down-stream zone, e.g. Zone 3 for the Relay 4, since the fault current does not pass through Zone 4 and therefore, the differential current component detected by the Relay 4 is zero. Details of a study that demonstrates the inability of protecting a microgrid based on differential current components can be found in [3]. In addition to inability for protecting against down-stream SLG faults, the relays do not detect a differential current component for LL faults in any of the microgrid protection zones, Fig. 1.

An alternative solution is to protect a microgrid against SLG and LL faults based on symmetrical current components [4]. A broad range of studies have been conducted on the AEP microgrid and it was concluded that SLG faults in down-stream zones of relays and all LL faults can be detected based on symmetrical current components. The SLG

and LL faults are detected from the zero-sequence component and the negative-sequence components of currents, respectively. However, zero- and negative-sequence components of current are also non-zero under normal operating conditions of a microgrid. This is due to the fact that a microgrid may, in general, include single-phase loads or three-phase unbalanced loads.

A study has been conducted for the AEP microgrid, in which the values of zero- and negative-sequence components of currents flowing through all relays of the microgrid were obtained for a maximum unbalanced load power of 20 percents. To ensure that the microgrid protection does not command for a trip under unbalanced load conditions, a threshold was assigned for each of the symmetrical current components. With the thresholds being set for all relays, each of them commands for breaker trip only when the corresponding zero-sequence or negative-sequence component exceeds a threshold. This guarantees that the protection system clears the SLG and LL faults in all protective zones while it does not command for an unwanted trip under unbalanced load conditions.

Based on the studies carried out for differential and symmetrical current components, a symmetric approach for protecting a microgrid against all SLG and LL faults has been developed. The developed microgrid protection approach employs the differential and zero-sequence current components as primary protection against SLG faults and the negative-sequence current component as a primary protection for LL faults.

If the microgrid primary protection fails, the time integral of current, i.e. I^2t, as a back-up protects the microgrid for all classes of fault [5]. A secondary back-up for the protection system is the conventional over-current protection. The over-current (I_{max}) protection usually commands for a trip after the I^2t protection, except for extremely high-current faults for which the over-current protection detects a fault fast. It is to be noted that, the I^2t and over-current protections are also back-up for the static switch in case that it fails to trip based on differential and symmetrical current protections.

In the following sections, first, structure of the AEP microgrid and its protection zones are described. Then, the results obtained for the symmetrical current components related to unbalanced load conditions and SLG and LL faults in all protection zones are presented. Coordination of the protective relays of the AEP microgrid, based on the results obtained for symmetrical current components, are also discussed. The results of studies carried out on the AEP microgrid for SLG and LL faults in all protection zones of the microgrid are presented. Conclusions are stated in the last section of the report.

2. AEP CERTS Microgrid

Fig. 1 shows a single-line representation of the AEP CERTS microgrid. The microgrid includes three microsources, specified as A_1, A_2 and B_1, and three local loads, specified as L_1, L_2 and L_3. Each microsource can provide a maximum output power of 60 kW and each load can consume a power up to a maximum amount of 120 kW, where the total load of microgrid should not exceed 180 kW. The microgrid is connected through a fast

semiconductor switch, that is called static switch, to the main grid. The combination of microgrid and the main grid has six protection zones that are specified as Zone 1 to Zone 6, Fig. 1.

CERTS Microgrid has two critical components, the static switch and the microsource. The static switch has the ability to autonomously island the microgrid from disturbances such as faults, IEEE 1547 events or power quality events. After islanding, the reconnection of the microgrid is achieved autonomously after the tripping event is no longer present. This synchronization is achieved by using the frequency difference between the islanded microgrid and the utility grid insuring a transient free operation without having to match frequency and phase angles at the connection point. Each microsource can seamlessly balance the power on the islanded microgrid using a power vs. frequency droop controller. This frequency droop also insures that the microgrid frequency is different from the grid frequency to facilitate reconnection to the utility.

To enhance reliability, a peer-to-peer and plug-and-play model is used for each component of the microgrid. The peer-to-peer concept insures that there are no components, such as a master controller or central storage unit that is critical for operation of the microgrid. This implies that the microgrid can continue operating with loss of any component or generator. With one additional source, (N+1), we can insure complete functionality with the loss of any source. Plug-and-play implies that a unit can be placed at any point on the electrical system without re-engineering the controls thereby reducing the chance for engineering errors. The plug-and-play model facilitates placing generators near the heat loads thereby allowing more effective use of waste heat without complex heat distribution systems such as steam and chilled water pipes.

Peer-to-peer and plug-and-play concepts also impact the protection design. The peer-to-peer concept insures that there are no protection components, such as a master coordinator or communication system critical to the protection of the microgrid. Plug-and-play implies that a unit can be placed at any point on the electrical system without re-engineering the protection thereby reducing the chance for engineering errors. This implies that microgrid protection is part of each source.
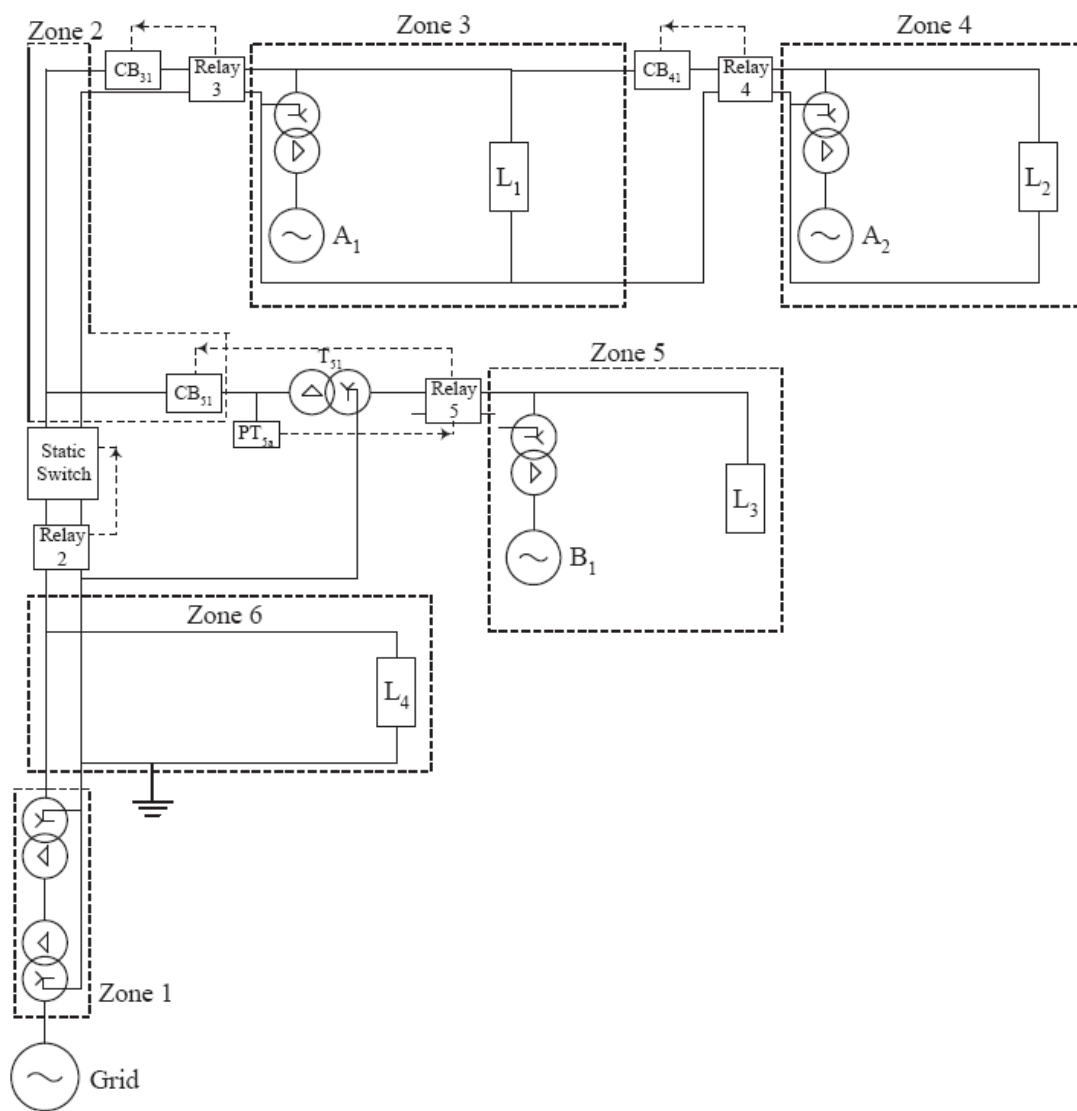
Figure 1: Schematic representation of the AEP CERTS microgrid

3. Basic Protection Issues

In general, a microgrid can operate in both the grid-connected mode and the islanded mode where the microgrid is interfaced to the main power system by a fast semiconductor switch called static switch, (SS). It is essential to protect a microgrid in both the grid-connected and the islanded modes of operation against all types of faults. The major issue arises in island operation with inverter-based sources. Inverter fault currents are limited by the ratings of the silicon devices to around 2 p.u. rated current. Fault currents in islanded inverter based microgrids may not have adequate magnitudes to use traditional over-current protection techniques. This possibility requires an expanded protection strategy.

The philosophy for protection is to have the same protection strategies for both islanded and grid-connected operation. The static switch is designed to open for all faults. With the static switch open, faults within the microgrid need to be cleared with techniques that do not rely on high fault currents. Fig. 1 shows a simple microgrid. The SS (static switch) separates the utility from the microgrid. The islanded part contains two loads and the inverter based sources. The microgrid assumes that the sources have adequate ratings to meet the load demands while in island mode. This example shows two sources in series with impedances between the sources using a four-wire configuration with a common ground point and one source in parallel.

In this example, we assume four protection zones with circuit breakers between Zone 2 and Zone 3, Zone 3 and Zone 4 and between Zone 2 and Zone 5. The system could be designed without these circuit breakers but the protection zones remain the same. In either case, sources feeding the fault must shut down without communications. For example, for a fault in Zone 2 we would expect the SS in Zone 2 to open in ½ to 2 cycles, the circuit breakers between Zones 2-3, 3-4 and 2-5 to open with the inverter-based sources in all Zones shutting down. If the fault was in Zone 4, ideally the SS would open and the circuit breaker between Zones 3 and 4 would open but the breaker between Zones 2 and 3 would not. The source in Zone 4 would also shut down. This would result in Zone 2, Zone 3 and Zone 5 operating as an island.

3.1. Single Line-to-Ground (SLG) Faults

The basic fault sensors for each zone are; a current sensors for each phase and a current sensor summing the three phases and the neutral in zones 2, 3 and 40. It was initially thought that a microgrid could be protected, at least for SLG faults, based on differential component of current I_d, ($I_d = \sum_{k=a,b,c,n} |I_k|$) for any number of sources in series. For example, in Fig.1, a SLG fault in Zone 4 would generate a non-zero differential current in zones 2, 3 and 4. This would result in Relay-2 opening the SS in ½ - 2 cycles followed by Relay-4 opening its circuit breaker and shutting down the source in Zone 4. Using a delay in Relay-3 would allow the section(s) of the microgrid up-stream of the fault to remain operating. This section could then reconnect to the utility autonomously since the faulted section is no longer connected. The problem with this concept is that any zones down-stream of the fault will not see the effect of ground currents. The I_d, sum of the three phase currents and neutral current, will be zero.

For example a SLG fault in Zone 3 will create differential current signals for the SS and Relay-3 to open and shut down the source in Zone 3, but the Zone 4 relay will not see the fault. The fault's ground current does not pass through Zone 4 and therefore, the differential current component detected by the Relay-4 is zero. This would leave Zones 3 and 4 energized as a faulted sub-island. For the case of a microgrid, which does not have breakers between zones, the SS would open and source in Zone 3 would be shut down but the source in Zone 4 would not shut down. It would continue to operate and feed the fault. If the fault were of high impedance, such back-up detection methods as over current and I^2t would not trip the source in Zone 4. Under-voltage protection could possible provide some back up, but again this would have problems. This problem requires using zero-sequence current detection for SLG faults. In this case, this is defined as the vector sum of the three phase currents.

As an example, consider the system in Fig.1 where the loads in all zones are 40 kW and the source in Zone 3 is dispatched at 40 kW and the Zones 4 and 5 are at 20 kW. The nominal line-to-line voltage is 480 volts. This implies that the grid provides 40 kW. When a high impedance SLG (~28 kW) fault is applied to phase A, in Zone 3, Relay-2 will see the fault, $I_d > 0$, and open the SS in 5-10 milliseconds. The resulting sequence voltages and currents seen by each relay are shown below;

FAULT CURRENTS SEEN BY THE RELAYS FOR A SLG FAULT IN ZONE 3 AND SS OPEN

Signal	Relay 2	Relay 3	Relay 4
$\lvert I_a \rvert (A)$	0	3.5	59.6
$\lvert I_b \rvert (A)$	0	20.8	4.8
$\lvert I_c \rvert (A)$	0	21.4	9.2
$I_d (A)$	0	**32.2**	0
$3\lvert I_0 \rvert (A)$	0	0	**54.4**
$\lvert V_+ \rvert (volts)$	391.6	392.1	391.2
$\lvert V_- \rvert (volts)$	0	4.8	5

Relay-4 has a 3-cycle delay to insure that the SS will open first. Relay 3 has a 10-cycle delay to insure that Zone 4 will shut down first. From the table, we see that Relay-4's differential current is zero but the zero sequence current provides the trip signal. Note that the voltage unbalance is small, (~1%) due to the local voltage control at each source. The usual relationship between the differential currents and the zero sequence currents is a function of the placement of the cts and the neutral conductors connection to the inverters' transformers.

Coordination between unbalanced loads and zero sequence currents is important. Unbalanced loads cause a zero sequence trip. The differential current detection does not see unbalanced loads.

17

3.2. Line-to-Line (L-to-L) Faults

Using I^2t protection for L-to-L faults is effective for low impedance faults but in many cases the time to trip will be long causing unnecessary disturbances to the loads and utility. High impedance fault current magnitudes will not be adequate to provide a trip. The our approach is to use negative sequence current to detect line-to-line faults.

Using the negative-sequence current, all L-to-L faults can be detected except the fault in Zone 3. In the microgrid of Fig. 1, no load exists between the static switch and Relay 3. When the static switch trips in response to a L-to-L fault in Zone 3, no current flows through Relay 3 and therefore, the relay does not command the corresponding breaker to trip. As a result, the microsource A_1 is not shut down and continues to provide the fault current.

4. Protection Based on Symmetrical Components

An SLG or LL fault imbalances phase currents of a number of protection zones of a microgrid. For the analysis of unbalanced currents, the concept of symmetrical components is usually employed [4]. The symmetrical components analysis uses a transformation matrix which converts phase components of an unbalanced three-phase current to equivalent positive-, negative- and zero-sequence current components [4]. The positive-sequence component represents a three-phase current that rotates in the same direction as the unbalanced three-phase current, while the negative-sequence component represents a three-phase current that rotates in an opposite direction with respect to the unbalanced three-phase currents. The zero-sequence component represents a system of three currents that have the same phase-angle.

An SLG fault generates usually zero- and negative-sequence current components, and an LL fault generates only a negative-sequence current component. The zero- and negative-sequence components of currents at the protective relays can be employed to detect SLG and LL faults in different protection zones of a microgrid. It is to be emphasized that zero- and negative-sequence current components are also generated and detected by relays under unbalanced load conditions. The microgrid concept is currently used for the distribution level of power systems which usually operates under unbalanced load conditions. Therefore, a protection approach based on symmetrical current components must distinguish between faulty and unbalanced operating conditions. In other words, the microgrid protection system must be coordinated such that it does not command for a trip under unbalanced load conditions while the protection system should detect SLG and LL faults in all zones of the microgrid.

For the AEP microgrid of Fig. 1, the zero- and negative-sequence components of currents at all relays, including Relay 2 that is attached to the static switch, are obtained for unbalanced load and SLG and LL fault conditions. The values of symmetrical current components are obtained based on digital-time domain simulations of the microgrid in the EMTP software environment. To comply with values measured by the real-world protective relays [6]-[8], magnitudes of all symmetrical components measured in the EMTP are multiplied by a factor of 3. Thus, each relay detects three times of the

magnitudes of symmetrical current components, i.e. $3|I_+|$, $3|I_-|$ and $3|I_0|$ which are referred to as magnitudes of positive, negative and zero components of currents herein after.

Magnitudes of the positive, negative and zero current components at all relays for a maximum load power unbalance of 20 percents and for SLG and LL faults in all protection zones have been obtained for the AEP microgrid and the results are presented in the following sections. For all the study cases, powers of the microsources A_1, A_2 and B_1 and powers of the loads L_1, L_2 and L_3 have been set at the following values: $P_{A1} = 40$ kW, $P_{A2} = 20$ kW, $P_{B1} = 0$ kW, $P_{L1} = 40$ kW, $P_{L2} = 60$ kW, and $P_{L3} = 40$ kW.

4.1. Unbalanced Load

In this case study, the phase resistances of load L_3 are changed such that it provides a power unbalance of 20 percents, while its total power remains at 60 kW. Table I gives the values of three-phase currents at the Relays 2, 3, 4 and 5 and magnitudes of the corresponding positive-, negative- and zero-sequence current components as well as the positive- and negative-sequence voltage components at all relays. It is seen from the results that the zero- and negative-sequence current components have maximum values of 11.9 and 26 A, respectively, and they correspond to the currents flowing through the Relay 4. If one of the other loads, i.e. L_1 or L_2, are 20 percents unbalanced, then current of the closest relay to the unbalanced load will have maximum zero- and negative-sequence components which do not exceed the maximum values obtained for the case of an unbalanced load L_3. When using symmetrical current components for detecting faults, the threshold of all relays must be selected above the maximum zero- and negative-sequence current magnitudes of 11.9 and 26 A. This ensures that the protection system does not trip any of the breakers when the AEP microgrid operates under a maximum load power unbalance of 20 percents.

TABLE I: SYMMETRICAL SEQUENCE CURRENT COMPONENTS AT THE AEP MICROGRID RELAYS FOR A 20 PERCENTS UNBALANCED LOAD L3

Device	$|I_a|$(A)	$|I_b|$(A)	$|I_c|$(A)	$3|I_+|$(A)	$3|I_-|$(A)	$3|I_0|$(A)	$|V_+|$(A)	$|V_-|$(A)
Relay 2	179.2	162.7	164.9	506.8	21.8	9.3	391.3	0.22
Relay 3	112.3	94.7	97.3	304.2	23.7	9.3	391.3	0.22
Relay 4	114	93.9	96.7	304.4	26	11.9	389.3	0.37
Relay 5	67.3	67.4	68.3	203	2	0	390.8	0.18

4.2. Single Line-to-Ground Fault

This section presents the results obtained from the EMTP based simulation of the AEP microgrid of Fig. 1 for an SLG fault in one of the protection Zones 2, 3, 4 and 5. The AEP microgrid operates under steady-state conditions with the source and load parameters given in Section 3. An SLG fault with a power of 28.5 kW ($R_f = 2.695$ Ohms) occurs in one of the protection zones at $t = 1$ s when the microgrid operates under steady-state conditions. Magnitudes of the phase currents, the symmetrical current components $3|I_+|$, $3|I_-|$ and $3|I_0|$ and the symmetrical voltage components $|V_+|$ and $|V_-|$ at all relays are

recorded when the microgrid operates under steady-state conditions subsequent to the SLG fault. Values of the parameters for the grid-connected (SS open) and the islanded (SS open) modes, when the static switch trips after the fault, are given in Tables II, III, IV and V for an SLG fault in Zones 4, 3, 2 and 5, respectively.

TABLE II: Symmetrical sequence current components at the AEP microgrid relays for an SLG fault in Zone 4

Device	$|I_a|$(A)	$|I_b|$(A)	$|I_c|$(A)	$3|I_+|$(A)	$3|I_-|$(A)	$3|I_0|$(A)	$|V_+|$(A)	$|V_-|$(A)
SS Closed								
Relay 2	211.6	117	116.9	445	102.8	88.1	391.3	1.05
Relay 3	147	47.6	50	242.7	112	88.1	391.3	1.05
Relay 4	158.8	42.4	42.7	242.8	123.3	111.4	389.6	1.76
Relay 5	66	66.3	70.7	202.9	9.2	0	390.9	0.88
SS Open								
Relay 2	0	0	0	0	0	0	391.6	0
Relay 3	2.4	20.8	21.6	33	40	0	392.1	4.5
Relay 4	81.5	4	8.5	72	88.4	85.4	391.1	5
Relay 5	13	11.6	24.4	33.2	40	0	392	3.8

TABLE III: Symmetrical sequence current components at the AEP microgrid relays for an SLG fault in Zone 3

Device	$|I_a|$(A)	$|I_b|$(A)	$|I_c|$(A)	$3|I_+|$(A)	$3|I_-|$(A)	$3|I_0|$(A)	$|V_+|$(A)	$|V_-|$(A)
SS Closed								
Relay 2	215.6	116.6	116.2	448	106.5	93.5	391.3	1.1
Relay 3	151.2	47.2	49.2	245.6	116	93.5	391.3	1.09
Relay 4	22.6	41.8	41.5	104.8	17	26	389.8	1.6
Relay 5	66	66.2	70.8	202.9	9.5	0	390.9	0.9
SS Open								
Relay 2	0	0	0	0	0	0	391.6	0
Relay 3	3.5	20.8	21.4	31.2	41.5	0	392.1	4.8
Relay 4	59.6	4.8	9.2	72	53	54.4	391.2	5
Relay 5	13	11.9	24.2	31.3	41.5	0	392	4.8

The results given in Tables II, III, IV and V indicate that magnitudes of zero-sequence current components of all relays that must trip for a close-by up-stream SLG fault are well above the maximum zero-sequence current component of 11.9 A that is related to the maximum load power unbalance of 20 percents. This means that a zero-sequence current threshold can be selected for all relays such that they can detect up-stream SLG faults in all microgrid protection zones. It is to be noted that the relays do not detect SLG faults that are located in their down-stream area after the static switch trips. However, the

down-stream faults are detected based on the differential current components at the relays.

TABLE IV: SYMMETRICAL SEQUENCE CURRENT COMPONENTS AT THE AEP MICROGRID RELAYS FOR AN SLG FAULT IN ZONE 2

Device	$|I_a|(A)$	$|I_b|(A)$	$|I_c|(A)$	$3|I_+|(A)$	$3|I_-|(A)$	$3|I_0|(A)$	$|V_+|(A)$	$|V_-|(A)$
SS Closed								
Relay 2	221.6	114.5	113.2	449	112	105.8	391.3	1.1
Relay 3	16	45	45.8	105	23.3	39.6	391.1	1.1
Relay 4	26.7	39.3	37.3	103.2	11.3	12.2	390.2	1.1
Relay 5	65.8	66.3	71	203	10	0	390.8	1.0
SS Open								
Relay 2	0	0	0	0	0	0	391.6	0
Relay 3	140.6	21.7	21.4	175.6	101.5	144.8	392	5
Relay 4	55	7.5	11.2	71.6	49.4	44.7	391.6	4.8
Relay 5	12.6	13.2	24.7	30.7	43.5	0	391.8	4.2

TABLE V: SYMMETRICAL SEQUENCE CURRENT COMPONENTS AT THE AEP MICROGRID RELAYS FOR AN SLG FAULT IN ZONE 5

Device	$|I_a|(A)$	$|I_b|(A)$	$|I_c|(A)$	$3|I_+|(A)$	$3|I_-|(A)$	$3|I_0|(A)$	$|V_+|(A)$	$|V_-|(A)$
SS Closed								
Relay 2	161.5	118.4	168.6	444	90.4	0	391.3	0.92
Relay 3	34.5	40.8	30.3	104.8	18.9	0	391.3	0.92
Relay 4	33.7	37.4	32.3	103.2	9.2	0	390.2	0.87
Relay 5	198	74.6	72.2	343.2	109.3	141.7	390.4	3
SS Open								
Relay 2	0	0	0	0	0	0	391.6	0
Relay 3	74.6	30.4	75.8	173	82	0	392	4
Relay 4	32.2	9.8	31.7	69.4	40	0	391.7	3.8
Relay 5	132	28.1	25.3	173.2	82.3	142	391.4	5.5

4.3. Line-to-Line Fault

This section presents the results obtained from the EMTP based simulation of the AEP microgrid of Fig. 1 for an LL fault in one of the protection Zones 2, 3, 4 and 5. The AEP microgrid operates under steady-state conditions with the source and load parameters given in Section 3. An LL fault with a power of 85.5 kW (R_f = 2.695 Ohms) occurs in one of the protection zones at $t = 1$ s when the microgrid operates under steady-state conditions. Magnitudes of the phase currents, the symmetrical current components $3|I_+|$, $3|I_-|$ and $3|I_0|$ and the symmetrical voltage components $|V_+|$ and $|V_-|$ at all relays are recorded when the microgrid operates under steady-state conditions subsequent to the LL fault. Values of the parameters for the grid-connected (SS closed) and the islanded (SS open) modes, when the static switch trips after the fault, are given in Tables VI, VII, VIII

21

and IX for an LL fault in Zones 4, 3, 2 and 5, respectively. The results indicate that magnitudes of negative-sequence current components of all relays that must trip for a close-by LL fault are well above the maximum negative-sequence current component of 26 A that is related to the maximum load power unbalance of 20 percents. In particular, magnitudes of the negative-sequence current components become much higher after the static switch trips. This means that a negative-sequence current threshold can be selected for all relays such that the AEP microgrid is protected against LL faults in all microgrid protection zones.

TABLE VI: SYMMETRICAL SEQUENCE CURRENT COMPONENTS AT THE AEP MICROGRID RELAYS FOR AN LL FAULT IN ZONE 4

Device	$|I_a|$(A)	$|I_b|$(A)	$|I_c|$(A)	$3|I_+|$(A)	$3|I_-|$(A)	$3|I_0|$(A)	$|V_+|$(A)	$|V_-|$(A)
SS Closed								
Relay 2	310	296	140	719	304	0	391	3.1
Relay 3	253	239	63.7	516	330	0	391	3.1
Relay 4	262	249	52.5	517	364	0	388.1	5.2
Relay 5	72	58.6	73.2	203	27	0	390.6	2.6
SS Open								
Relay 2	0	0	0	0	0	0	391.6	0
Relay 3	75	72	6.7	135	118	0	391.4	14
Relay 4	157	152	6.9	275	260	0	389.5	15
Relay 5	45.2	85	40	136	118	0	391.8	11

TABLE VII: SYMMETRICAL SEQUENCE CURRENT COMPONENTS AT THE AEP MICROGRID RELAYS FOR AN LL FAULT IN ZONE 3

Device	$|I_a|$(A)	$|I_b|$(A)	$|I_c|$(A)	$3|I_+|$(A)	$3|I_-|$(A)	$3|I_0|$(A)	$|V_+|$(A)	$|V_-|$(A)
SS Closed								
Relay 2	318	304	139	733	318	0	391	3.1
Relay 3	262	247	63	530	346	0	391	3.2
Relay 4	22.1	43.4	51.3	112	50.7	0	388.5	4.8
Relay 5	72.2	58.2	73.4	203	28.4	0	390.6	2.7
SS Open								
Relay 2	0	0	0	0	0	0	391.6	0
Relay 3	77.6	75	6.4	140	124	0	391.3	14
Relay 4	85.6	90	5.6	147	157	0	390	15
Relay 5	46.6	88	42	140	124	0	391.7	12

TABLE VIII: SYMMETRICAL SEQUENCE CURRENT COMPONENTS AT THE AEP MICROGRID RELAYS FOR AN LL FAULT IN ZONE 2

Device	$|I_a|$(A)	$|I_b|$(A)	$|I_c|$(A)	$3|I_+|$(A)	$3|I_-|$(A)	$3|I_0|$(A)	$|V_+|$(A)	$|V_-|$(A)
SS Closed								
Relay 2	324	309	135	737	335	0	390.9	3.4
Relay 3	21.6	41.6	58.2	109	70	0	390.9	3.4
Relay 4	27.8	34	45.8	105	34	0	389.8	3.2
Relay 5	72.3	57.8	74	203	30	0	390.5	2.8
SS Open								
Relay 2	0	0	0	0	0	0	391.6	0
Relay 3	170	172	4.5	290	302	0	390.8	15
Relay 4	83	85	2.3	145	147	0	390.8	14
Relay 5	47.2	90	44	142	130	0	391.4	12

TABLE IX: SYMMETRICAL SEQUENCE CURRENT COMPONENTS AT THE AEP MICROGRID RELAYS FOR AN LL FAULT IN ZONE 5

Device	$|I_a|$(A)	$|I_b|$(A)	$|I_c|$(A)	$3|I_+|$(A)	$3|I_-|$(A)	$3|I_0|$(A)	$|V_+|$(A)	$|V_-|$(A)
SS Closed								
Relay 2	327	196	222	716	266	0	390.9	2.7
Relay 3	22	53	41.1	109	55.6	0	390.9	2.7
Relay 4	26.6	42.1	37.6	105	27	0	389.8	2.6
Relay 5	280	270	99	616	322	0	389	8.8
SS Open								
Relay 2	0	0	0	0	0	0	391.6	0
Relay 3	173	85	89	276	242	0	391.2	12
Relay 4	85.2	43	43	138	117	0	391.2	11
Relay 5	151	148	11.5	276	242	0	390.1	16

5. Coordination of Protection

This section presents a summary of the items that are considered when the protection system of the AEP microgrid is coordinated. Based on the results presented in Section 3.1 and Section 3.2, a threshold of $3|I_0|$=35 A is selected for all relays for detecting a down-stream SLG fault based on a zero-sequence current component. The up-stream SLG faults that are close to a relay are detected based on a differential current component for which a threshold of $|I_d|$ =15 A is chosen. Also, based on the result presented in Section 3.1 and Section 3.3, a threshold of $3|I_-|$=95 A is considered for all relays when detecting an LL fault based on a negative-sequence current component. The thresholds considered for the symmetrical and differential current components guarantee that the protection system detects all SLG faults with a power more than 28.5 kW/phase and all LL faults with a power greater than 85.5 kW that occur in any of the microgrid protection zones.

To prevent detecting instantaneous or short faults and transients, a delay of 50 ms (3 cycles) is set for all relays before detecting an SLG or LL fault. In other words, if a

23

symmetrical component remains greater than the corresponding threshold longer than 50 ms, then the relay will command the corresponding circuit breaker to trip. The delay of 50 ms is considered for all relays except the Relay 3, for the case of SLG faults only, for which a delay of 167 ms (10 cycles) is chosen. The longer delay considered for the Relay 3 ensures that the relay does not command for a trip for SLG faults in Zone 4, Fig. 1, as such faults are cleared by the Relay 4 in less than 10 cycles. It is to be noted that the delay considered for detecting an LL fault by the Relay 3 is the same as that of the other relays, i.e. 50 ms. It should also be noted that no delay is considered for the SLG and LL faults that are detected by the Relay 2, that is attached to the static switch, since the switch is expected to clear a fault within a maximum period of 8 ms (half a cycle).

When a trip signal is sent by a relay to the corresponding breaker, a delay of 30 ms is considered before starting to open phase switches of the corresponding breaker. The reason for considering the delay of 30 ms is that magnitudes of the symmetrical current components of the relays have different rise times and thus, each of them exceeds the corresponding threshold at a different time than the others. If no delay is considered, one of the relays may not command for a necessary trip since the corresponding symmetrical component does not stay above the threshold more than 50 ms prior to the fault clearance by another breaker. This causes one of the microsources to continue its operation in a stand-alone mode after the fault clearance, which is not desirable. To ensure that all relays which are expected to command for a trip have sufficient time to detect a fault, the delay of 30 ms is considered before disconnecting a circuit breaker.

Once a symmetrical current component with a magnitude greater than the corresponding threshold lasts more than 3 cycles, the corresponding relay sends a trip command to the circuit breaker. The 3-cycle delay is considered for all relays, except the Relay 3 which has a 10-cycle delay for SLG faults, and the Relay 2 which has no delay for all types of fault. When the breaker receives a trip command, its controller considers a delay of 30 ms before starting the procedure of disconnecting the breaker phases. The 30 ms delay is considered for all the breakers except the static switch which has no delay. After a delay of 30 ms, the three-phase circuit breaker who has received a trip command is opened, one phase at a time. To open a circuit breaker, currents of all three phases of the breaker are measured and when a phase current crosses zero, the corresponding phase switch is opened. The disconnection procedure is the same for all the breakers including the static switch.

TABLE X: Relay settings

Protection	Relay	Up-stream SLG faults	Down-stream SLG faults	Line-to-Line faults
Primary	2	$I_d > 15A$ delay=0 ms	$3\|I_0\| > 35A$ delay=0 ms	$3\|I_-\| > 95A$ Delay=0 ms
	3	$I_d > 15A$ delay=167 ms	$3\|I_0\| > 35A$ delay=167 ms	$3\|I_-\| > 95A$ delay=50 ms
	4	$I_d > 15A$ delay=50 ms	$3\|I_0\| > 35A$ delay=50 ms	$3\|I_-\| > 95A$ Delay=50 ms
	5	$I_d > 15A$ delay=50 ms	$3\|I_0\| > 35A$ delay=50 ms 50% volts dip	$3\|I_-\| > 95A$ Delay=50 ms
1st Back-up	2	I^2t activation level $\|I\| > 480A$		
	3	I^2t activation level $\|I\| > 225A$		
	4	I^2t activation level $\|I\| > 125A$		
	5	I^2t activation level $\|I\| > 125A$		
2nd Back-up and under voltage protection	2	Peak current $\|I\| > 750A$	Voltage power quality levels	
	3		50% under voltage delay 30 cycles	
	4		50% under voltage delay 20 cycles	
	5		50% under voltage delay 20 cycles	

6. Study Cases

This section evaluates performance of the protection system of the AEP microgrid based on digital time-domain simulation studies in the EMTP software environment. Performance of the protection system is studied for SLG and LL faults in all the microgrid protection zones, i.e. Zones 2, 3, 4, 5 and 6 of Fig. 1. All SLG and LL faults have a resistance of 2.695 Ohms which corresponds to a 28.5 kW/phase power for SLG faults and a 85.5 kW power for LL faults, respectively. The fault resistance is equal to the resistance used for experimenting faults at the real-world microgrid test site in Ohio.

For all study cases of this section, powers of the microsources A_1, A_2 and B_1 and powers of the loads L_1, L_2 and L_3 are set at the following values: $P_{A1} = 40$ kW, $P_{A2} = 20$ kW, $P_{B1} = 10$ kW, $P_{L1} = 40$ kW, $P_{L2} = 40$ kW, and $P_{L3} = 40$ kW. For each study case, the results are shown in four figures and each figure shows the operating parameters related to the relay that is attached to the static switch or one of the Relays 3, 4 and 5. Each figure shows the three-phase voltages and currents, the real and reactive components of power, and the frequency at one of the relays. Each figure also shows normalized magnitudes of the differential and zero- and negative-sequence current components

measured at a relay as well as the relay output signal that can command a breaker to trip or to continue its operation. The figure that corresponds to the Relay 5 also shows normalized magnitude of the phase voltage that is measured at the delta side of the transformer T_{51}, Fig. 1. The phase voltage is measured for detecting SLG faults in Zone 2 for which the Relay 5 does not detect a differential or zero-sequence current component.

6.1. SLG Faults

SLG Fault in Zone 4

The AEP microgrid of Fig. 1 is operating at steady-state conditions with the source and load settings as explained in Section 5 and an SLG fault with a resistance of 2.695 Ohms is applied in Zone 4 at t=1.0 s. Figs. 3(a)-(e) to Figs. 6(a)-(e) show variations of the three-phase voltages and currents, the real and reactive power components, and the frequencies measured at the Relays 2, 3, 4 and 5, respectively, in response to the SLG fault.

Fig. 2(f) shows that the Relay 2 commands the static switch to trip right after the fault since the relay detects a differential current component that exceeds 1.0 pu (15 A). Fig. 3(f) shows that the Relay 3 does not command for a trip since it has a built-in delay of 10 cycles and magnitude of the differential current component detected by the relay falls below 1.0 pu before 10 cycle when the breaker CB_{41} clears the fault. Fig. 4(f) shows that the Relay 4 sends a trip command to the circuit breaker CB_{41} since magnitudes of both the differential and zero-sequence current components at the relay are greater than 1.0 pu for a period more than 50 ms (3 cycles). However, the relay trip command is due to the differential current component since it exceeds 1.0 pu earlier than the zero-sequence current component. Fig. 5(f) shows that the Relay 5 does not command for a trip since none of its fault detection parameters, i.e. the differential and symmetrical current components, exceed the threshold of 1.0 pu.

For the case of SLG fault in Zone 4, the static switch islands the microgrid and the breaker CB_{41} disconnects Zone 4 of the microgrid and shuts down the microsource A_2. The Zones 2, 3 and 5 of the microgrid and the microsources A_1 and B_1 continue the operation subsequent to the fault detection and its clearance. The results shown in Fig. 2 to Fig. 5 demonstrate that the developed protection system is able to protect the AEP microgrid against an SLG fault in Zone 4 with a power of 28.5 kW/phase by clearing the fault and isolating the microgrid from the main grid. Since the fault current increases as the fault power increases, it is concluded that the microgrid protection system is able to protect all SLG faults in Zone 4 with a power more than or equal to 28.5 kW/phase.

Figure 2 : Response of the Relay 2 to a 28.5 kW SLG fault in Zone 4: (a,b) three-phase voltages and currents, (c,d) real and reactive power components, (e) frequency, and (f) differential and zero- and negative-sequence current components and output command of the relay

Figure 3: Response of the Relay 3 to a 28.5 kW SLG fault in Zone 4: (a,b) three-phase voltages and currents, (c,d) real and reactive power components, (e) frequency, and (f) differential and zero- and negative-sequence current components and output command of the relay

Figure 4: Response of the Relay 4 to a 28.5 kW SLG fault in Zone 4: (a,b) three-phase voltages and currents, (c,d) real and reactive power components, (e) frequency, and (f) differential and zero- and negative-sequence current components and output command of the relay
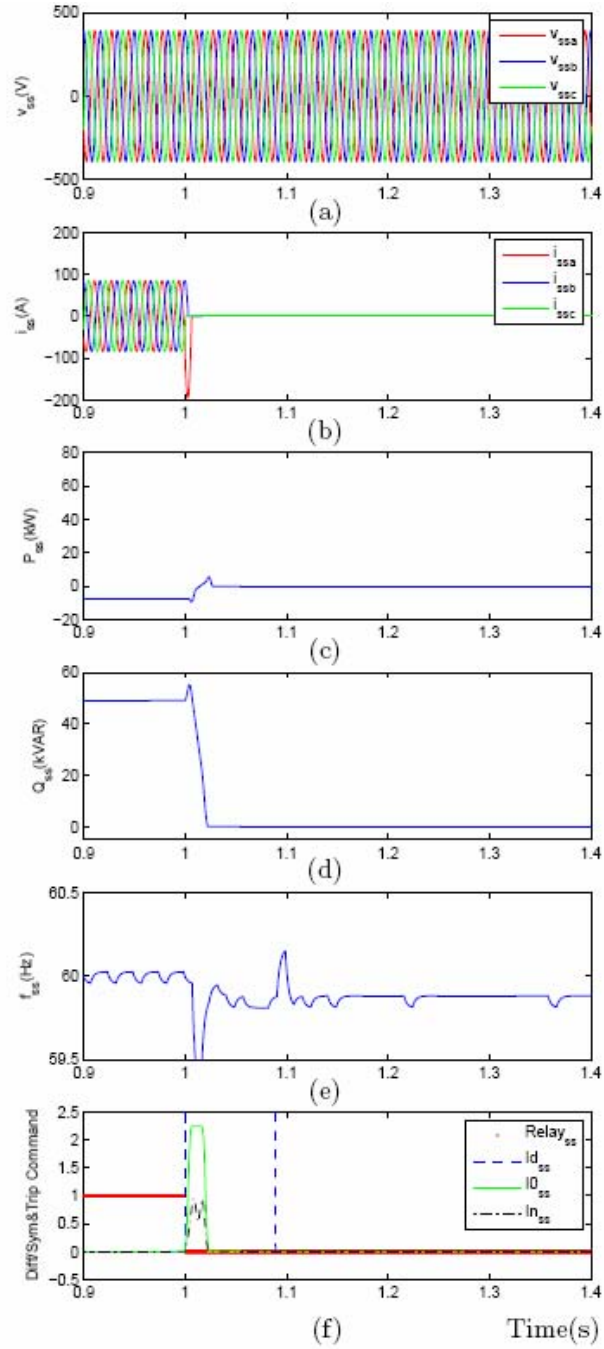
Figure 5: Response of the Relay 5 to a 28.5 kW SLG fault in Zone 4: (a,b) three-phase voltages and currents, (c,d) real and reactive power components, (e) frequency, and (f) differential and zero- and negative-sequence current components, negative-sequence voltage component at the transformer T_{51} and output command of the relay

SLG Fault in Zone 3

The AEP microgrid of Fig. 1 is operating at steady-state conditions with the source and load settings as explained in Section 0.5 and an SLG fault with a resistance of 2.695 Ohms is applied in Zone 3 at t=1.0 s. Figs. 7(a)-(e) to Figs. 10(a)-(e) show variations of the three-phase voltages and currents, the real and reactive power components, and the frequencies measured at the Relays 2, 3, 4 and 5, respectively, in response to the SLG fault.

Fig. 6(f) shows that the Relay 2 commands the static switch to trip right after the fault since the relay detects a differential current component that exceeds 1.0 pu (15 A). Fig. 7(f) shows that the Relay 3 commands for a trip since even when the circuit breaker CB_{41} trips, the fault is not cleared in the protection Zone 3 and the relay still detects a differential current component. Fig. 8(f) shows that the Relay 4 sends a trip command to the circuit breaker CB_{41} since magnitude of the zero-sequence current component at the relay is greater than 1.0 pu (35 A) for a period more than 50 ms (3 cycles). Fig. 9(f) shows that the Relay 5 does not command for a trip since none of its fault detection parameters, i.e. the differential and symmetrical current components, exceeds the threshold of 1.0 pu.

For the case of SLG fault in Zone 3, the static switch islands the microgrid and the breakers CB_{31} and CB_{41} disconnect Zones 3 and 4 of the microgrid and shut down the microsources A_1 and A_2. The Zones 2 and 5 of the microgrid and the microsource B_1 continue the operation subsequent to the fault detection and its clearance. The results shown in Fig. 6 to Fig. 9 demonstrate that the developed protection system is able to protect the AEP microgrid against an SLG fault in Zone 3 with a power of 28.5 kW/phase by clearing the fault and isolating the microgrid from the main grid. Since the fault current increases as the fault power increases, it is concluded that the microgrid protection system is able to protect all SLG faults in Zone 3 with a power more than or equal to 28.5 kW/phase.

Figure 6: Response of the Relay 2 to a 28.5 kW SLG fault in Zone 3: (a,b) three-phase voltages and currents, (c,d) real and reactive power components, (e) frequency, and (f) differential and zero- and negative-sequence current components and output command of the relay
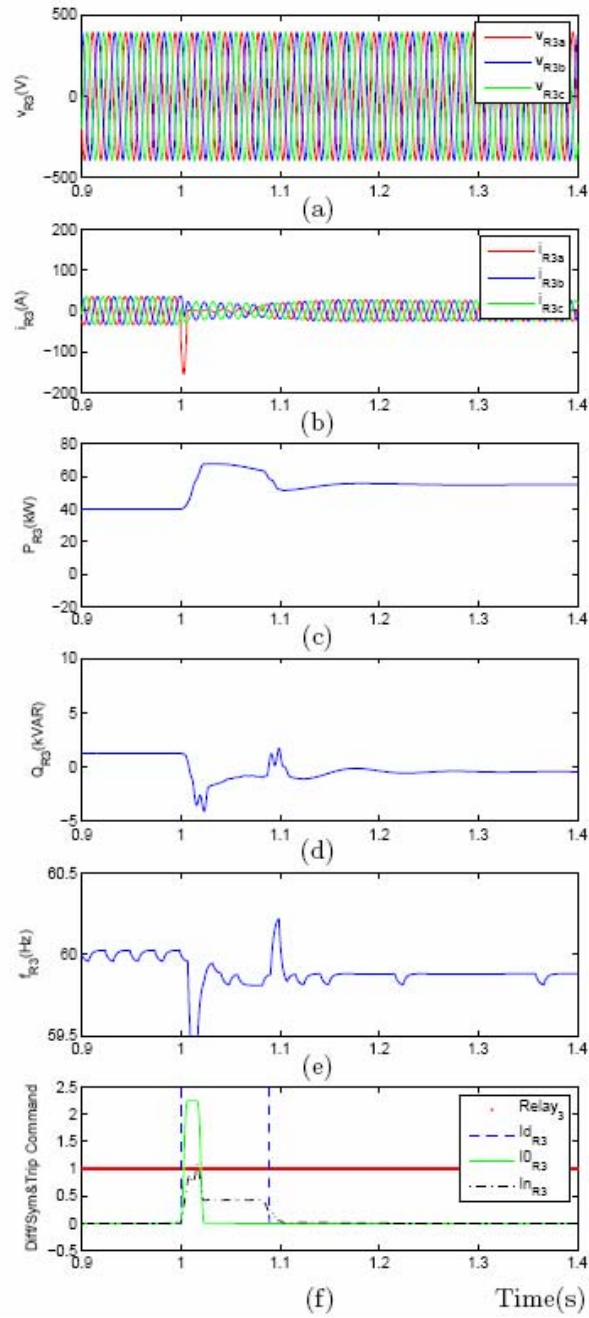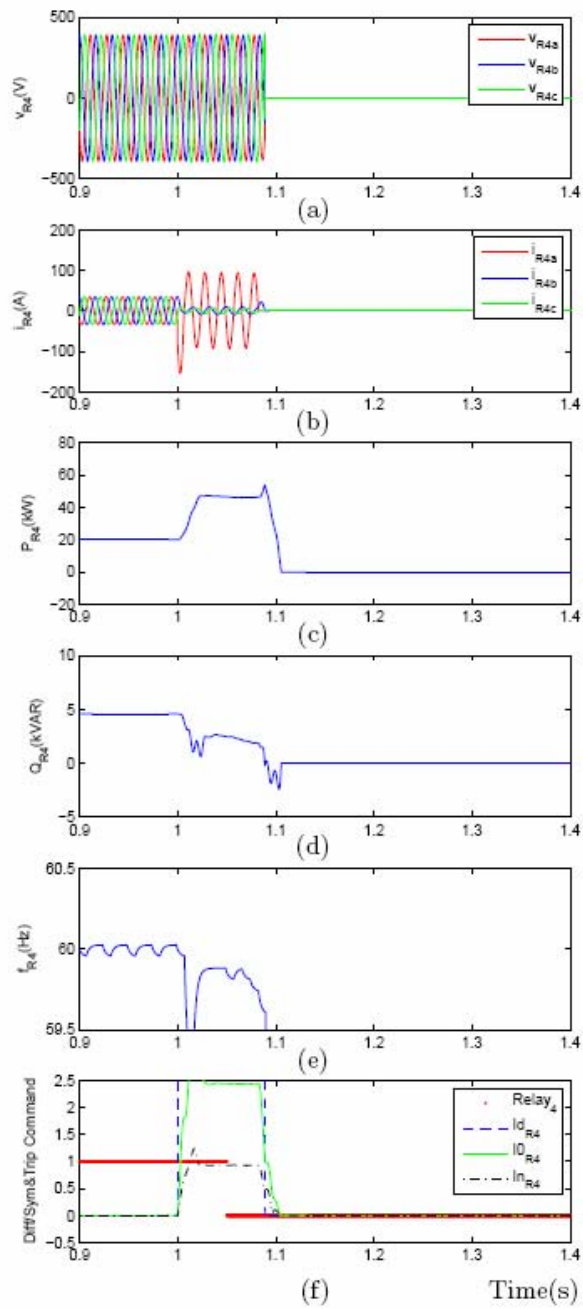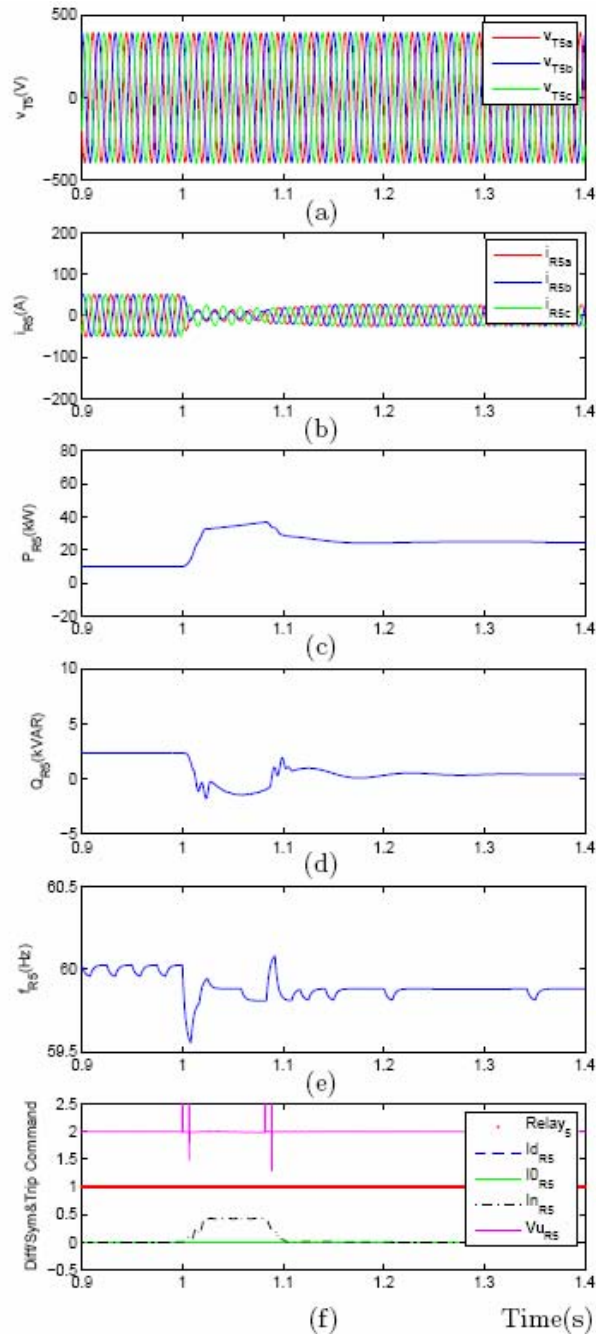
Figure 7: Response of the Relay 3 to a 28.5 kW SLG fault in Zone 3: (a,b) three-phase voltages and currents, (c,d) real and reactive power components, (e) frequency, and (f) differential and zero- and negative-sequence current components and output command of the relay

Figure 8: Response of the Relay 4 to a 28.5 kW SLG fault in Zone 3: (a,b) three-phase voltages and currents, (c,d) real and reactive power components, (e) frequency, and (f) differential and zero- and negative-sequence current components and output command of the relay
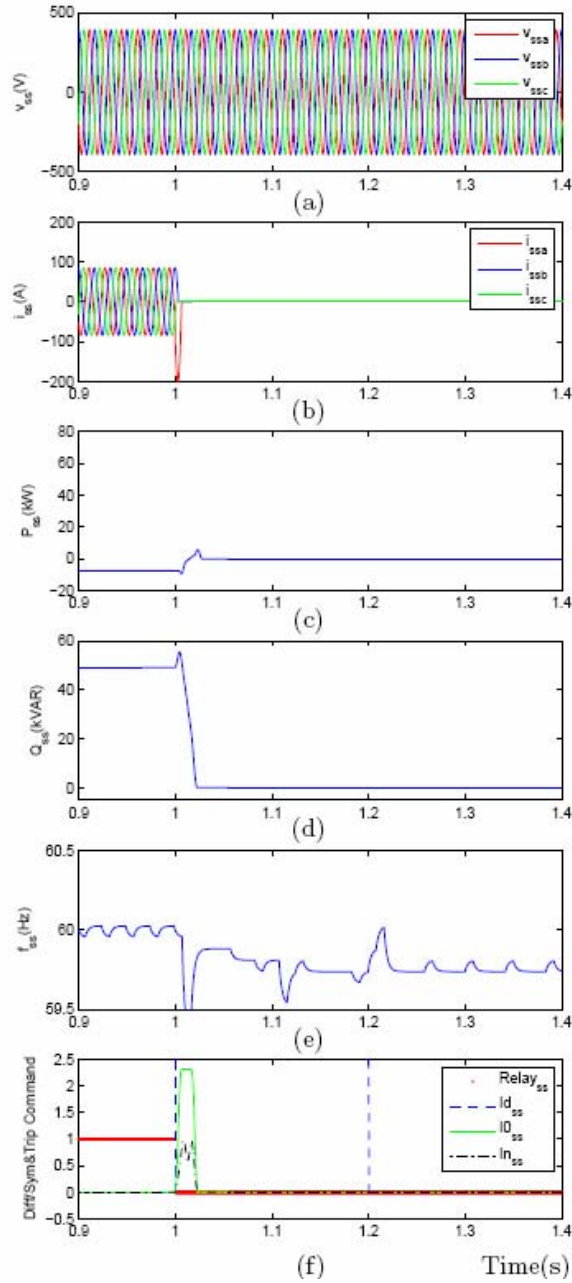
Figure 9: Response of the Relay 5 to a 28.5 kW SLG fault in Zone 3: (a,b) three-phase voltages and currents, (c,d) real and reactive power components, (e) frequency, and (f) differential and zero- and negative-sequence current components, negative-sequence voltage component at the transformer T_{51} and output command of the relay

SLG Fault in Zone 2

The AEP microgrid of Fig. 1 is operating at steady-state conditions with the source and load settings as explained in Section 5 and an SLG fault with a resistance of 2.695 Ohms is applied in Zone 2 at t=1.0 s. Figs. 11(a)-(e) to Figs. 14(a)-(e) show variations of the three-phase voltages and currents, the real and reactive power components, and the frequencies measured at the Relays 2, 3, 4 and 5, respectively, in response to the SLG fault.

Fig. 10(f) shows that the Relay 2 commands the static switch to trip right after the fault since the relay detects a differential current component that exceeds 1.0 pu (15 A). Fig. 11(f) shows that the Relay 3 sends a trip command to the circuit breaker CB_{31} since magnitude of the negative-sequence current component at the relay is greater than 1.0 pu (95 A) for a period more than 50 ms (3 cycles). Fig. 12(f) shows that the Relay 4 sends a trip command to the circuit breaker CB_{41} since magnitude of the zero-sequence current component at the relay is greater than 1.0 pu (35 A) for a period more than 50 ms. Fig. 13(f) shows that the Relay 5 sends a trip command to the circuit breaker CB51 since magnitude of the phase voltage at the delta-side of transformer T_{51} falls below 1.0 pu (196 V) for a period more than 20 cycles.

For the case of SLG fault in Zone 2, the static switch islands the microgrid and the breakers CB_{31}, CB_{41} and CB_{51} disconnect all three zones of the microgrid and shut down all the microsource located inside the microgrid. The results shown in Fig. 10 to Fig. 13 demonstrate that the developed protection system is able to protect the AEP microgrid against an SLG fault in Zone 2 with a power of 28.5 kW/phase by clearing the fault and isolating the microgrid from the main grid. Since the fault current increases as the fault power increases, it is concluded that the microgrid protection system is able to protect all SLG faults in Zone 2 with a power more than or equal to 28.5 kW/phase.

Figure 10: Response of the Relay 2 to a 28.5 kW SLG fault in Zone 2: (a,b) three-phase voltages and currents, (c,d) real and reactive power components, (e) frequency, and (f) differential and zero- and negative-sequence current components and output command of the relay
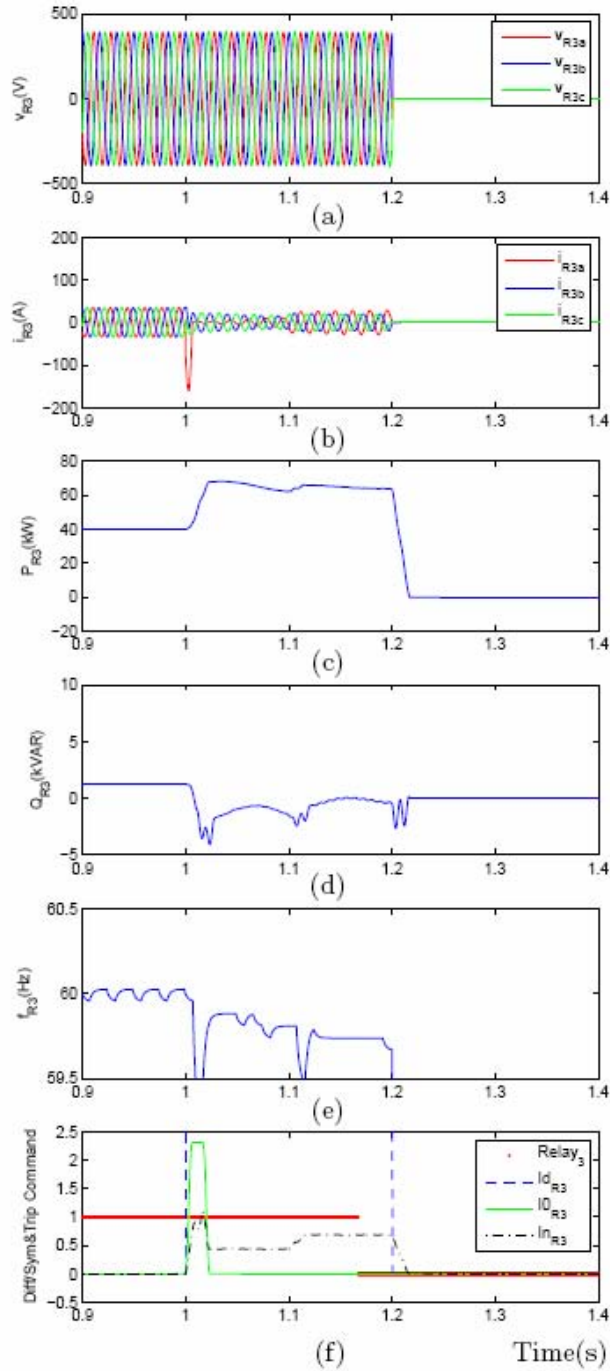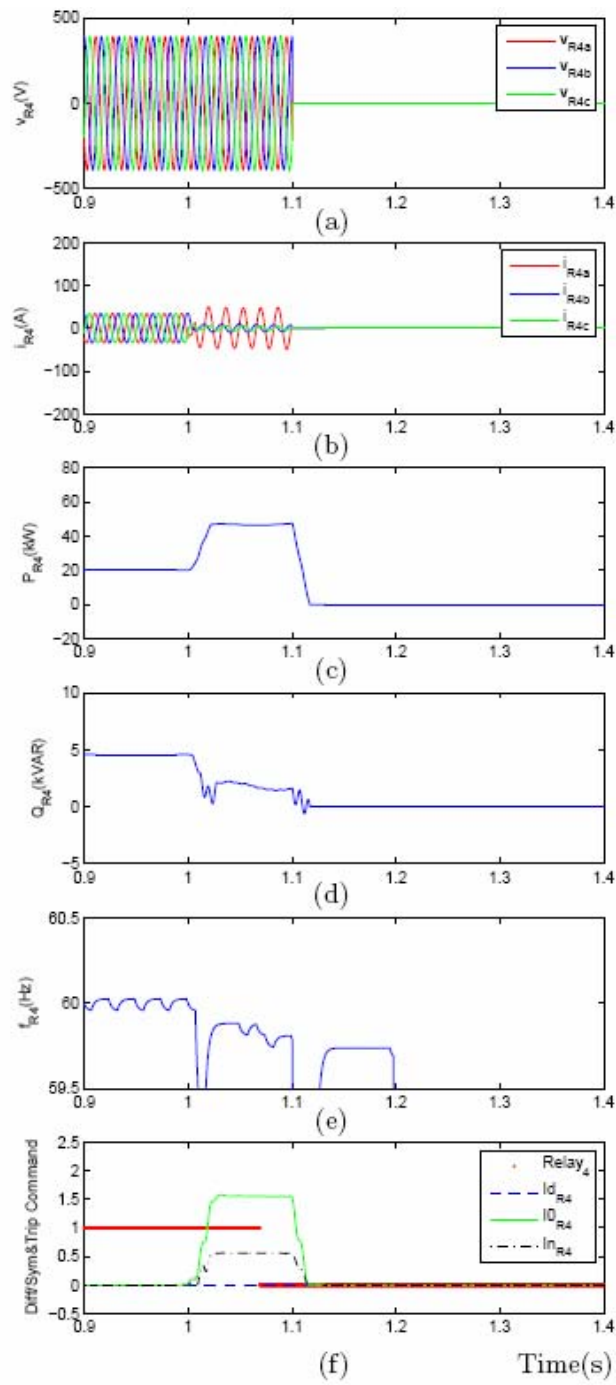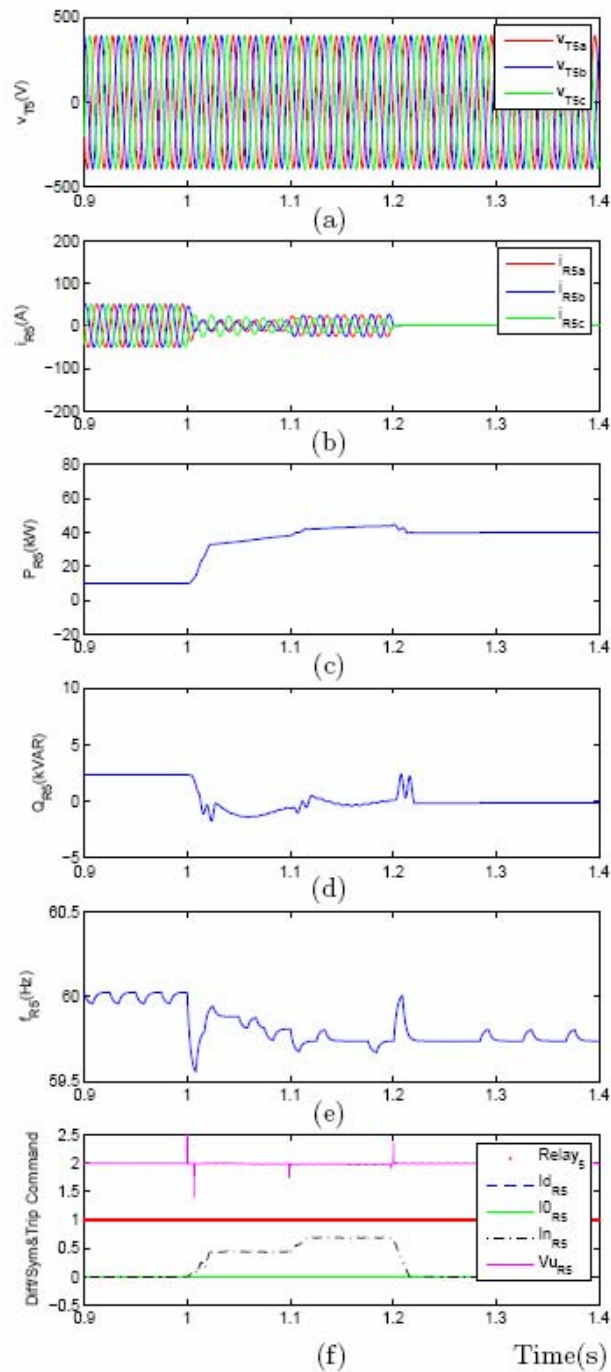
Figure 11: Response of the Relay 3 to a 28.5 kW SLG fault in Zone 2: (a,b) three-phase voltages and currents, (c,d) real and reactive power components, (e) frequency, and (f) differential and zero- and negative-sequence current components and output command of the relay

Figure 12: Response of the Relay 4 to a 28.5 kW SLG fault in Zone 2: (a,b) three-phase voltages and currents, (c,d) real and reactive power components, (e) frequency, and (f) differential and zero- and negative-sequence current components and output command of the relay
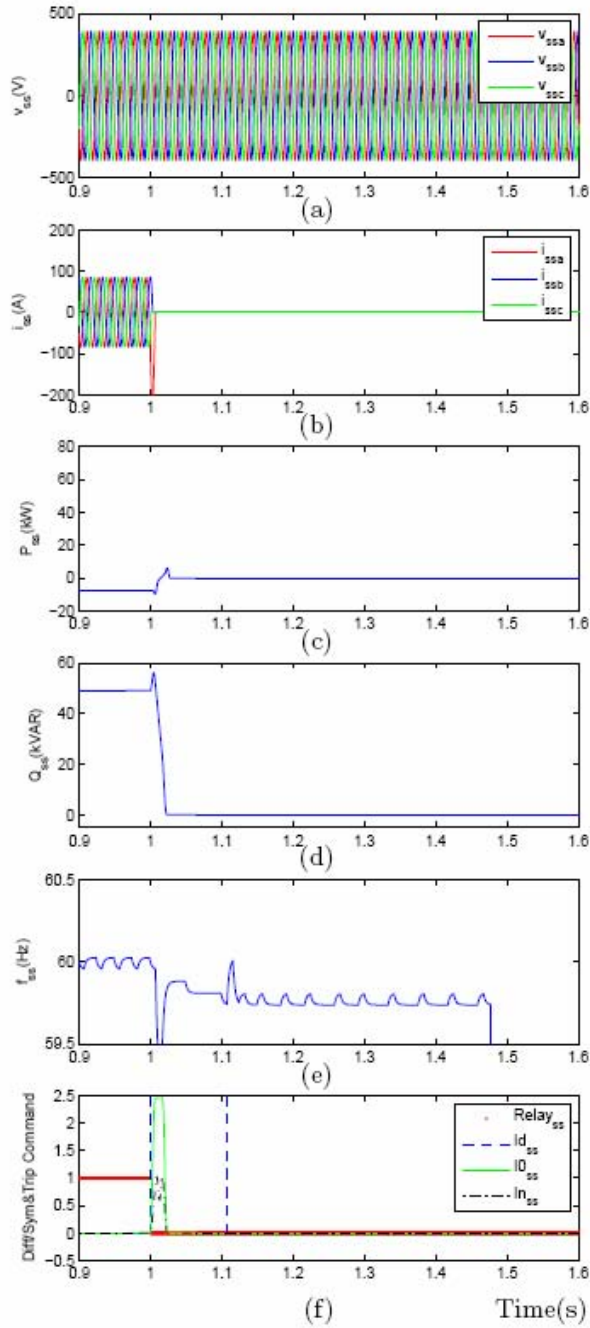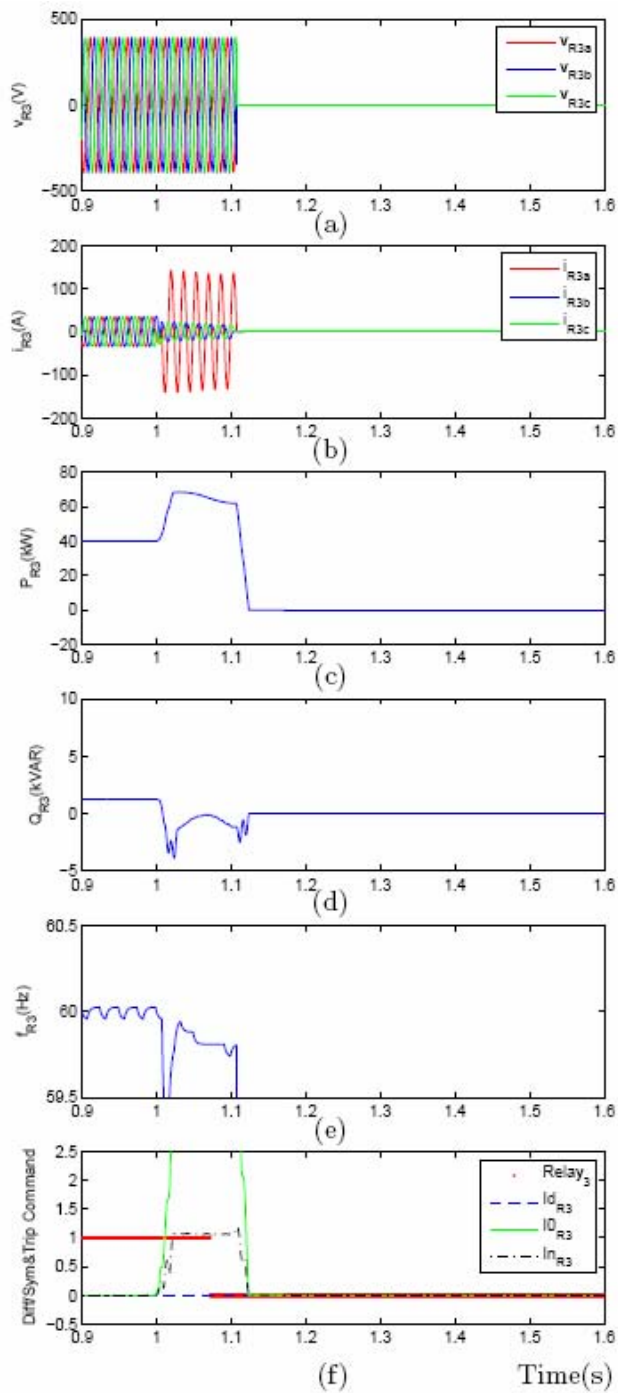
Figure 13: Response of the Relay 5 to a 28.5 kW SLG fault in Zone 2: (a,b) three-phase voltages and currents, (c,d) real and reactive power components, (e) frequency, and (f) differential and zero- and negative-sequence current components, negative-sequence voltage component at the transformer T_{51} and output command of the relay

SLG Fault in Zone 5

The AEP microgrid of Fig. 1 is operating at steady-state conditions with the source and load settings as explained in Section 5 and an SLG fault with a resistance of 2.695 Ohms is applied in Zone 5 at t=1.0 s. Figs. 15(a)-(e) to Figs. 18(a)-(e) show variations of the three- phase voltages and currents, the real and reactive power components, and the frequencies measured at the Relays 2, 3, 4 and 5, respectively, in response to the SLG fault.

Fig. 14(f) shows that the Relay 2 commands the static switch to trip when CB_{51} trips since the relay detects an instantaneous negative-sequence current component that exceeds 1.0 pu (95 A). Fig. 15(f) shows that the Relay 3 does not command for a trip since none of its fault detection parameters, i.e. the differential and symmetrical current components, exceeds the threshold of 1.0 pu. Fig. 16(f) shows that the Relay 4 does not command for a trip since none of its fault detection parameters, i.e. the differential and symmetrical current components, exceeds the threshold of 1.0 pu. Fig. 17(f) shows that the Relay 5 commands for a trip to the circuit breaker CB_{51} since magnitude of the differential current component at the relay is above the threshold of 1.0 pu (15 A) for a period more than 50 ms.

For the case of SLG fault in Zone 5, the static switch islands the microgrid and the breaker CB_{51} disconnects Zone 5 of the microgrid and shuts down the microsource B_1. The Zones 2, 3 and 4 of the microgrid and the microsources A_1 and A_2 continue the operation subsequent to the fault detection and its clearance. The results shown in Fig. 14 to Fig.17 demonstrate that the developed protection system is able to protect the AEP microgrid against an SLG fault in Zone 5 with a power of 28.5 kW/phase by clearing the fault and isolating the microgrid from the main grid. Since the fault current increases as the fault power increases, it is concluded that the microgrid protection system is able to protect all SLG faults in Zone 5 with a power more than or equal to 28.5 kW/phase.

Figure 14: Response of the Relay 2 to a 28.5 kW SLG fault in Zone 5: (a,b) three-phase voltages and currents, (c,d) real and reactive power components, (e) frequency, and (f) differential and zero- and negative-sequence current components and output command of the relay
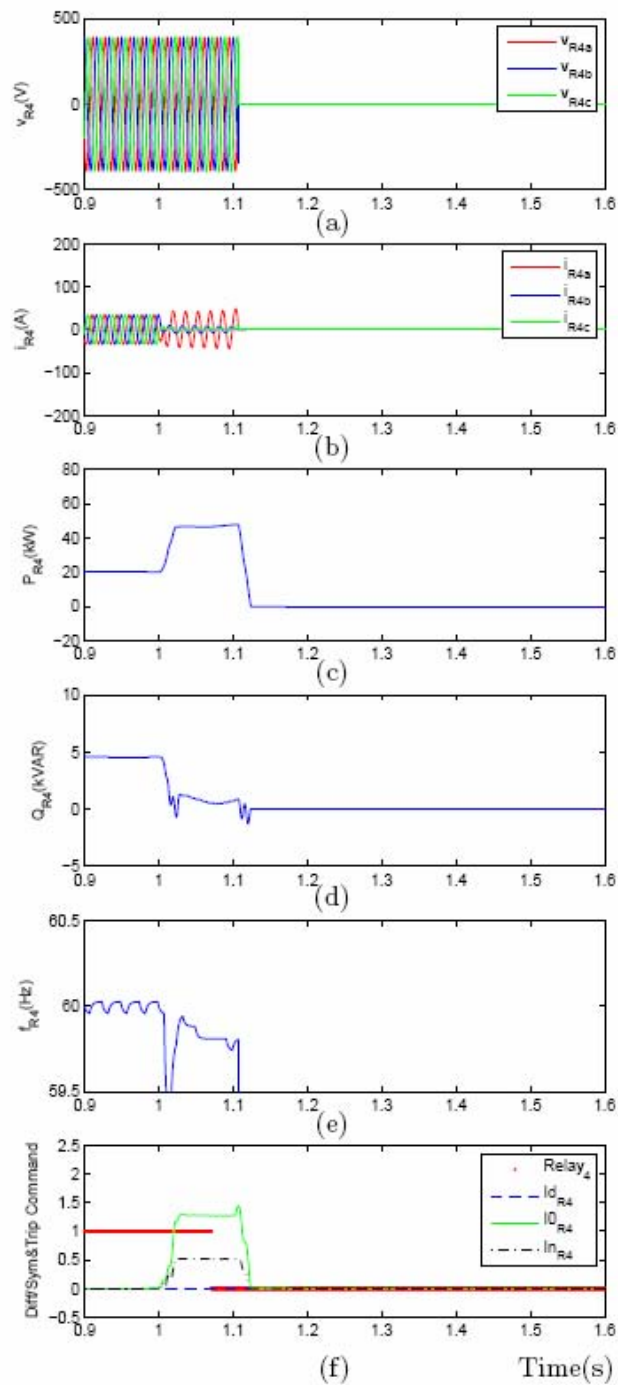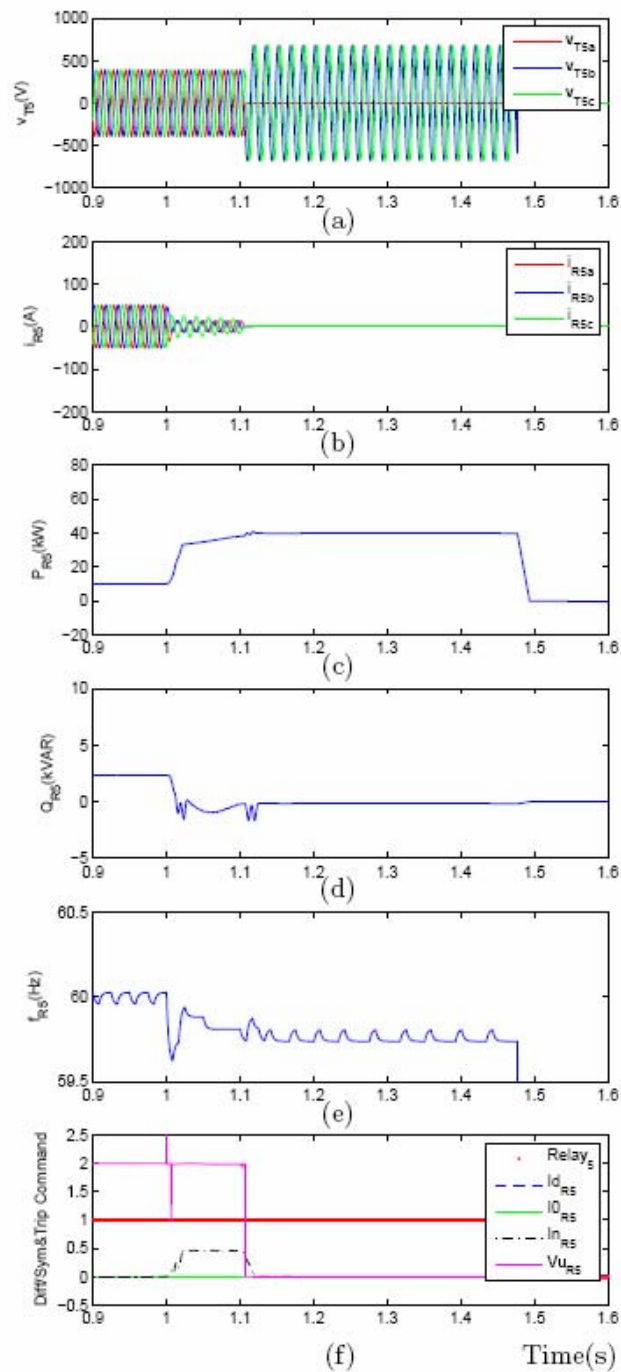
42

Figure 15: Response of the Relay 3 to a 28.5 kW SLG fault in Zone 5: (a,b) three-phase voltages and currents, (c,d) real and reactive power components, (e) frequency, and (f) differential and zero- and negative-sequence current components and output command of the relay
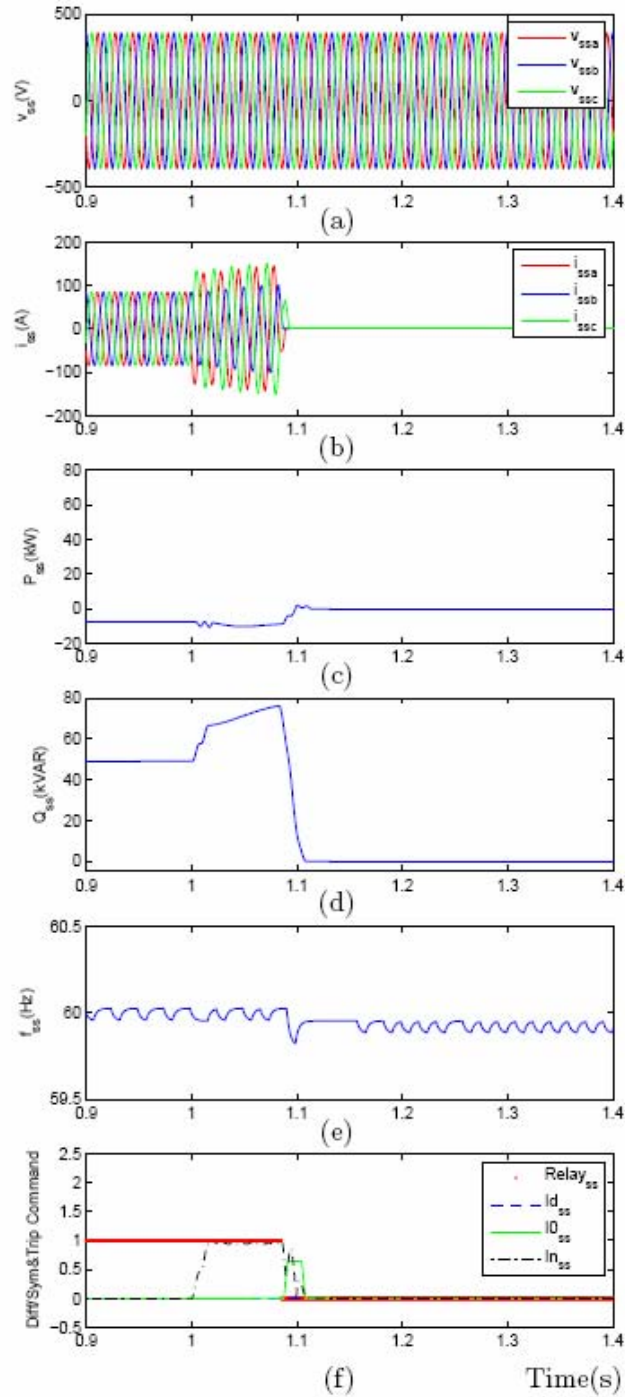
Figure 16: Response of the Relay 4 to a 28.5 kW SLG fault in Zone 5: (a,b) three-phase voltages and currents, (c,d) real and reactive power components, (e) frequency, and (f) differential and zero- and negative-sequence current components and output command of the relay
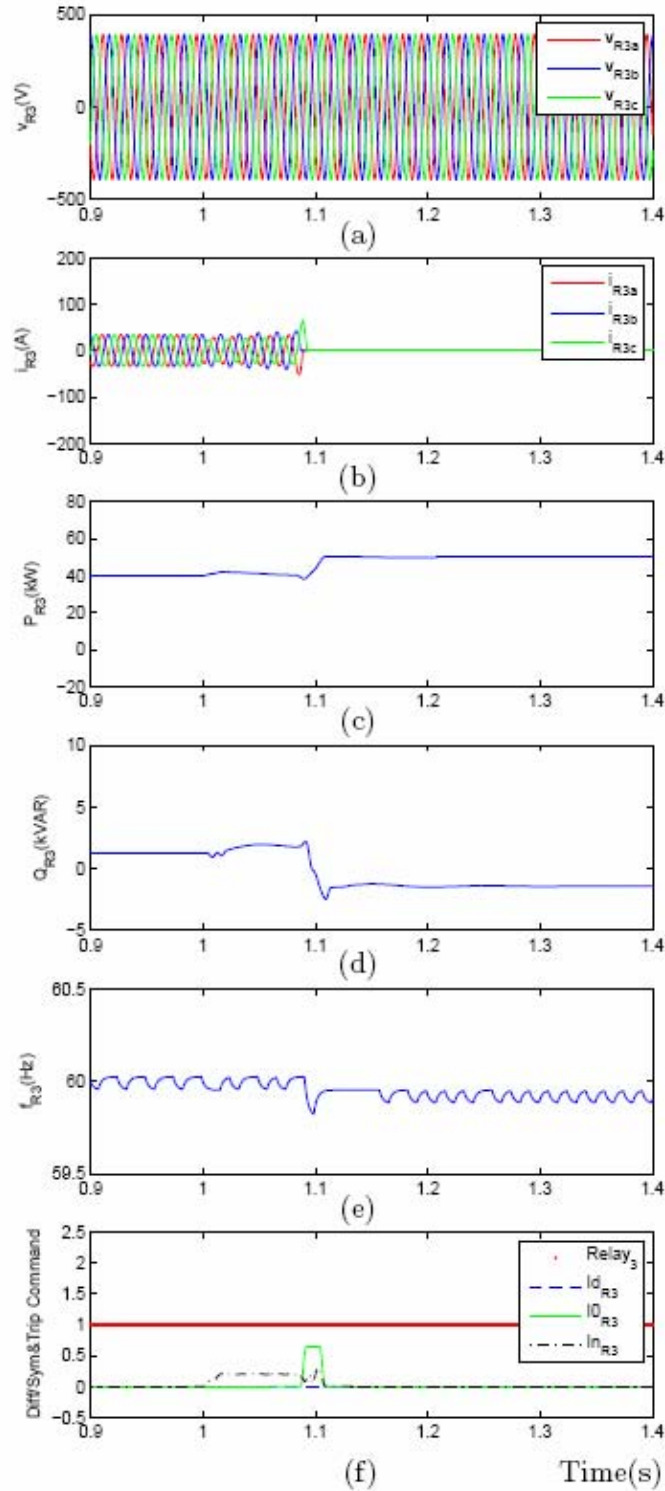
Figure 17: Response of the Relay 5 to a 28.5 kW SLG fault in Zone 5: (a,b) three-phase voltages and currents, (c,d) real and reactive power components, (e) frequency, and (f) differential and zero- and negative-sequence current components, negative-sequence voltage component at the transformer T_{51} and output command of the relay

SLG Fault in Zone 6

The AEP microgrid of Fig. 1 is operating at steady-state conditions with the source and load settings as explained in Section 5 and an SLG fault with a resistance of 2.695 Ohms is applied in Zone 6 at t=1.0 s. Figs. 19(a)-(e) to Figs. 22(a)-(e) show variations of the three- phase voltages and currents, the real and reactive power components, and the frequencies measured at the Relays 2, 3, 4 and 5, respectively, in response to the SLG fault.

Fig. 18(f) shows that the Relay 2 commands the static switch to trip since the relay detects an instantaneous negative-sequence current component that exceeds 1.0 pu (95 A). Fig. 19(f) shows that the Relay 3 does not command for a trip since none of its fault detection parameters, i.e. the differential and symmetrical current components, exceeds the threshold of 1.0 pu. Fig. 20(f) shows that the Relay 4 does not command for a trip since none of its fault detection parameters, i.e. the differential and symmetrical current components, exceeds the threshold of 1.0 pu. Fig. 21(f) shows that the Relay 5 does not command for a trip since none of its fault detection parameters, i.e. the differential and symmetrical current components, exceeds the threshold of 1.0 pu.

For the case of SLG fault in Zone 6, the static switch islands the microgrid. The Zones 2, 3, 4 and 5 of the microgrid and the microsources A_1, A_2 and B_1 continue the operation subsequent to the fault detection and its clearance. The results shown in Fig. 18 to Fig. 21 demonstrate that the developed protection system is able to protect the AEP microgrid against an SLG fault in Zone 6 with a power of 28.5 kW/phase by isolating the microgrid from the main grid. Since the fault current increases as the fault power increases, it is concluded that the microgrid protection system is able to protect all SLG faults in Zone 6 with a power more than or equal to 28.5 kW/phase.

Figure 18: Response of the Relay 2 to a 28.5 kW SLG fault in Zone 6: (a,b) three-phase voltages and currents, (c,d) real and reactive power components, (e) frequency, and (f) differential and zero- and negative-sequence current components and output command of the relay
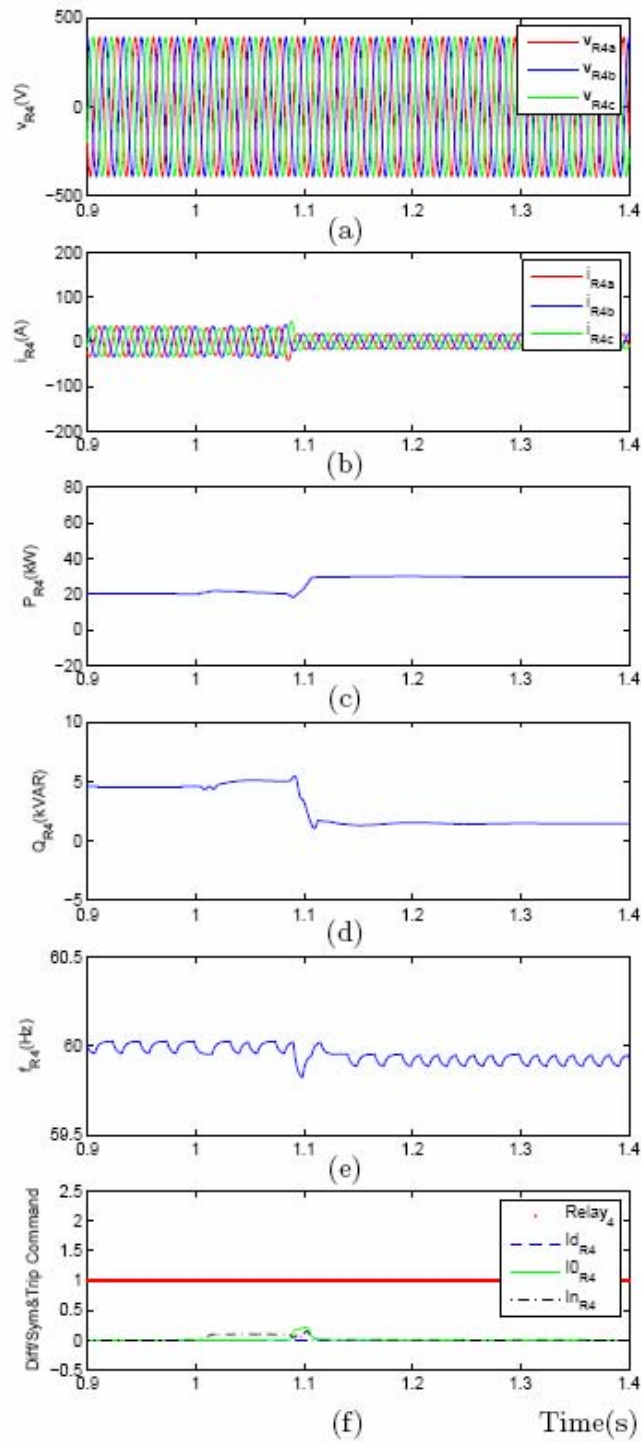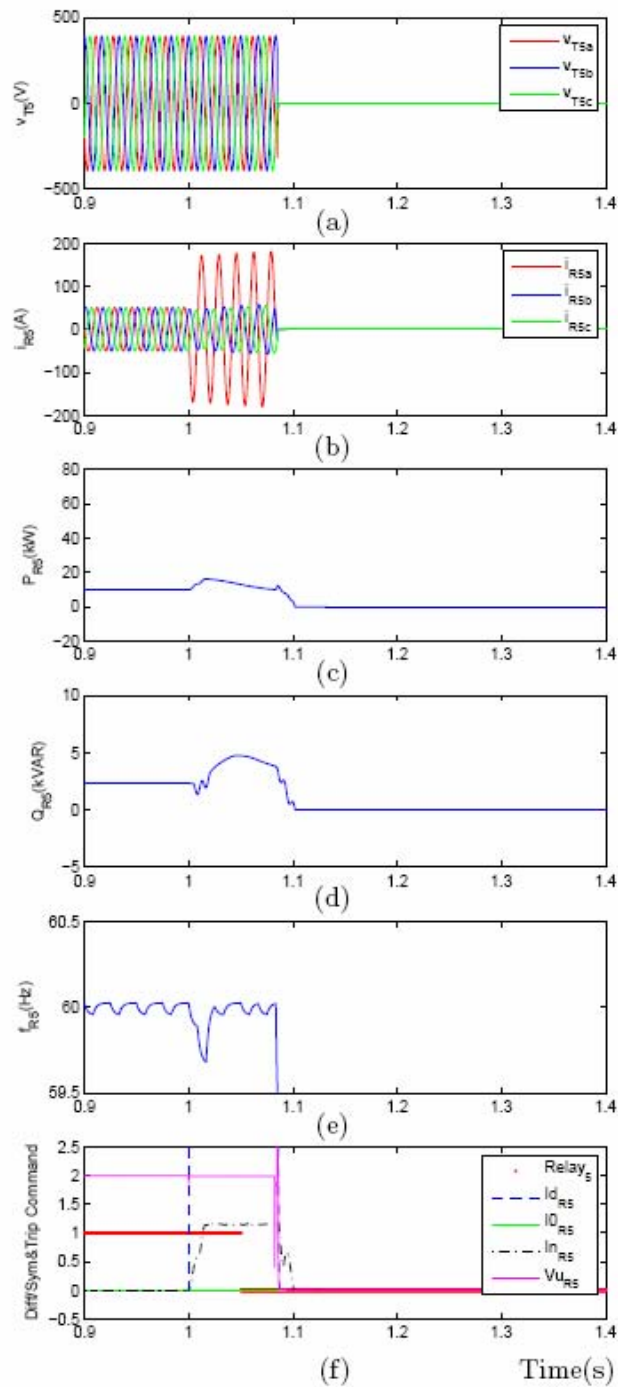
47

 Figure 19: Response of the Relay 3 to a 28.5 kW SLG fault in Zone 6: (a,b) three-phase voltages and currents, (c,d) real and reactive power components, (e) frequency, and   (f) differential and zero- and negative-sequence current components and output command of the relay
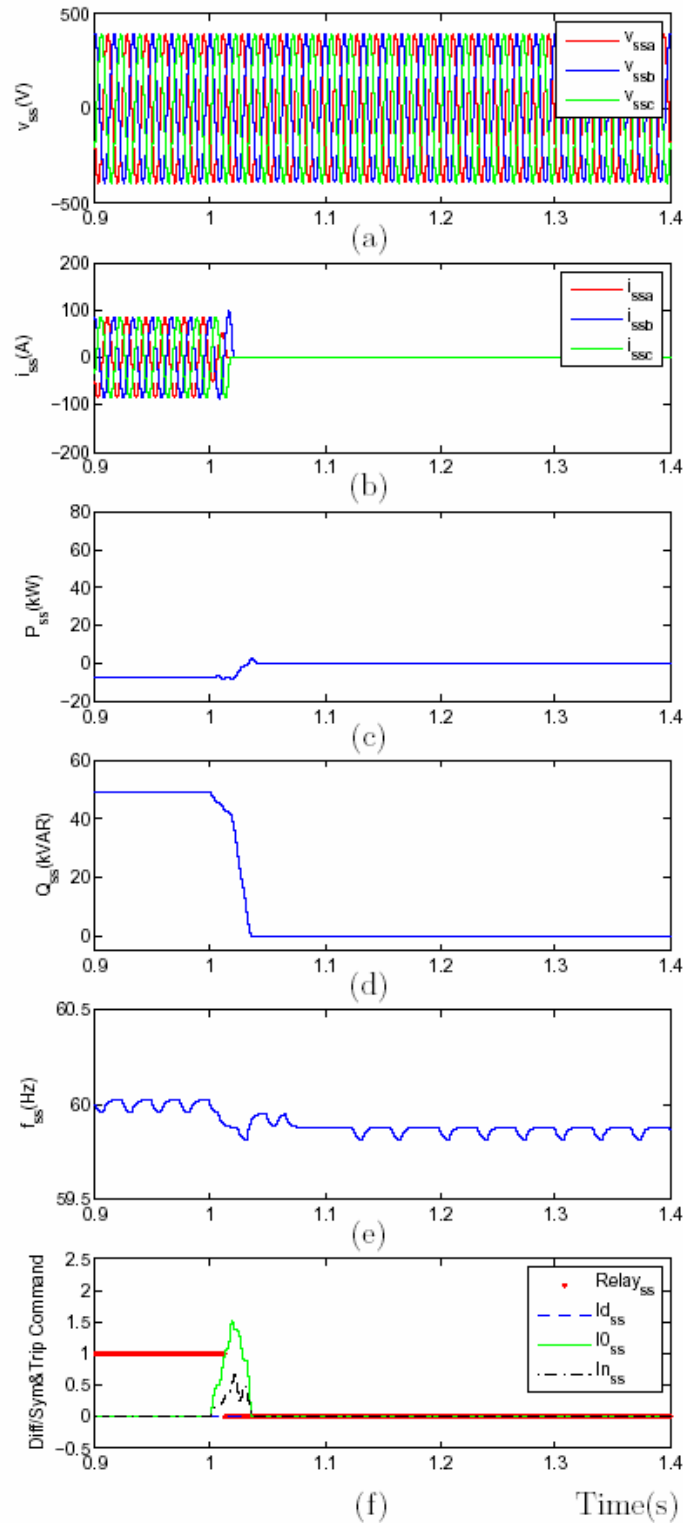
Figure 20: Response of the Relay 4 to a 28.5 kW SLG fault in Zone 6: (a,b) three-phase voltages and currents, (c,d) real and reactive power components, (e) frequency, and (f) differential and zero- and negative-sequence current components and output command of the relay
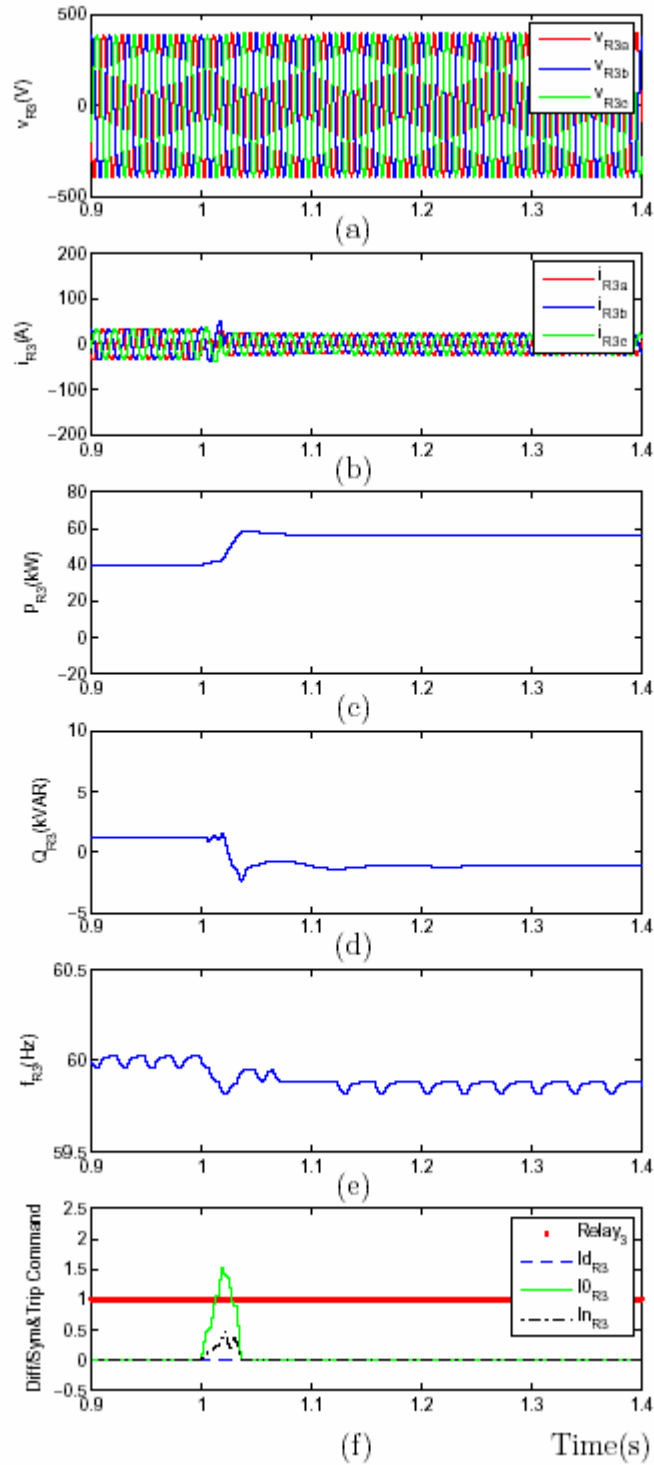
49

Figure 21: Response of the Relay 5 to a 28.5 kW SLG fault in Zone 6: (a,b) three-phase voltages and currents, (c,d) real and reactive power components, (e) frequency, and (f) differential and zero- and negative-sequence current components, negative-sequence voltage component at the transformer T_{51} and output command of the relay

6.2. Line-to-Line Faults

Line-to-Line Fault in Zone 4

The AEP microgrid of Fig. 1 is operating at steady-state conditions with the source and load settings as explained in Section 5 and an LL fault with a resistance of 2.695 Ohms is applied in Zone 4 at t=1.0 s. Figs. 23(a)-(e) to Figs. 26(a)-(e) show variations of the three-phase voltages and currents, the real and reactive power components, and the frequencies measured at the Relays 2, 3, 4 and 5, respectively, in response to the LL fault.

Fig. 22(f) shows that the Relay 2 commands the static switch to trip shortly after the fault when the relay detects a negative-sequence current component that exceeds 1.0 pu (95 A). Fig. 23(f) shows that the Relay 3 commands CB_{31} to trip since magnitude of the negative-sequence current component at the relay is above 1.0 pu for a period more than 50 ms (3 cycles). Fig. 24(f) shows that the Relay 4 sends a trip command to the circuit breaker CB_{41} since magnitude of the negative-sequence current component at the relay is greater than 1.0 pu for a period more than 50 ms. Fig. 25(f) shows that the Relay 5 commands CB_{51} to trip since magnitude of the negative-sequence current component at the relay is above 1.0 pu for a period more than 50 ms. Magnitudes of the differential and zero-sequence current components of all relays do not exceed the corresponding threshold of 15 A and 35 A.

For the case of an LL fault in Zone 4, the static switch islands the microgrid and the breakers CB_{31}, CB_{41} and CB_{51} disconnects all zones of the microgrid and shut down all the microsource located inside the microgrid. The results shown in Fig. 22 to Fig. 25 demonstrate that the developed protection system is able to protect the AEP microgrid against an LL fault in Zone 4 with a power of 85.5 kW by clearing the fault and disconnecting all protection zones of the microgrid. Since the fault current increases as the fault power increases, it is concluded that the microgrid protection system is able to protect all LL faults in Zone 4 with a power more than or equal to 85.5 kW.

Figure 22: Response of the Relay 2 to a 85.5 kW LL fault in Zone 4: (a,b) three-phase voltages and currents, (c,d) real and reactive power components, (e) frequency, and (f) differential and zero- and negative-sequence current components and output command of the relay
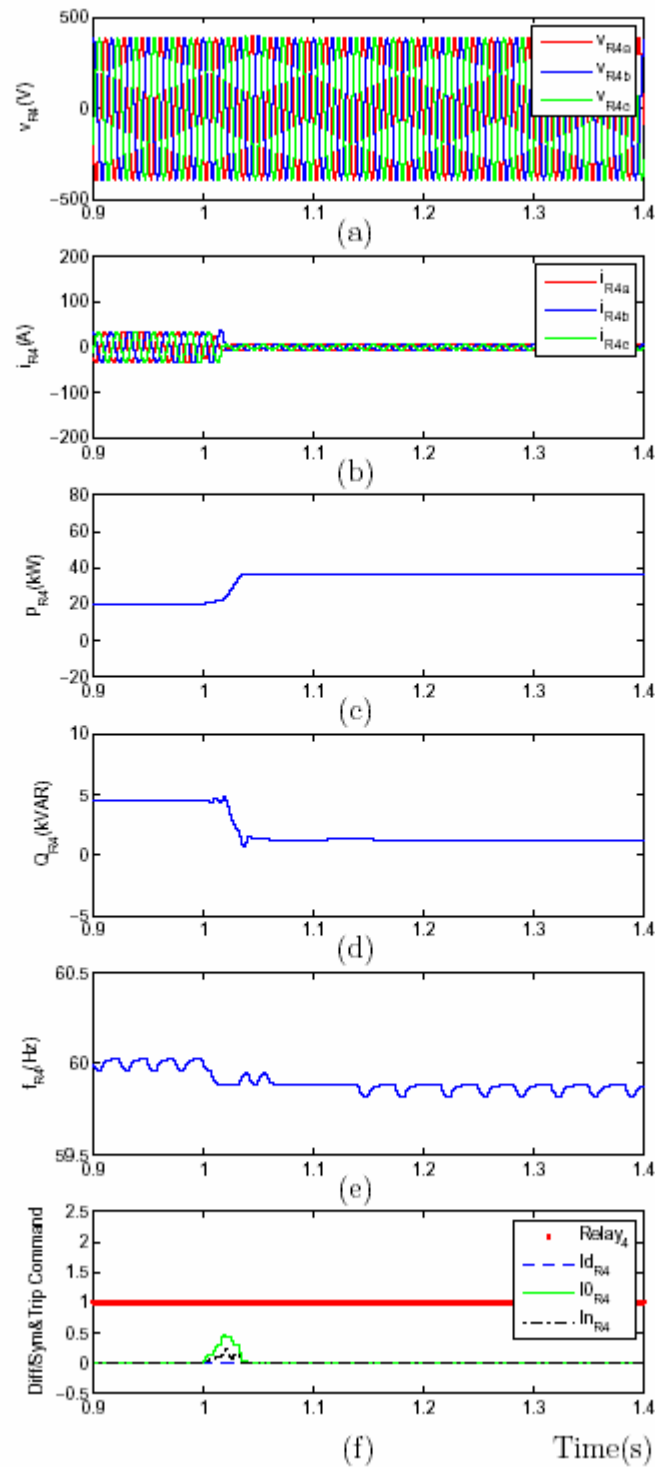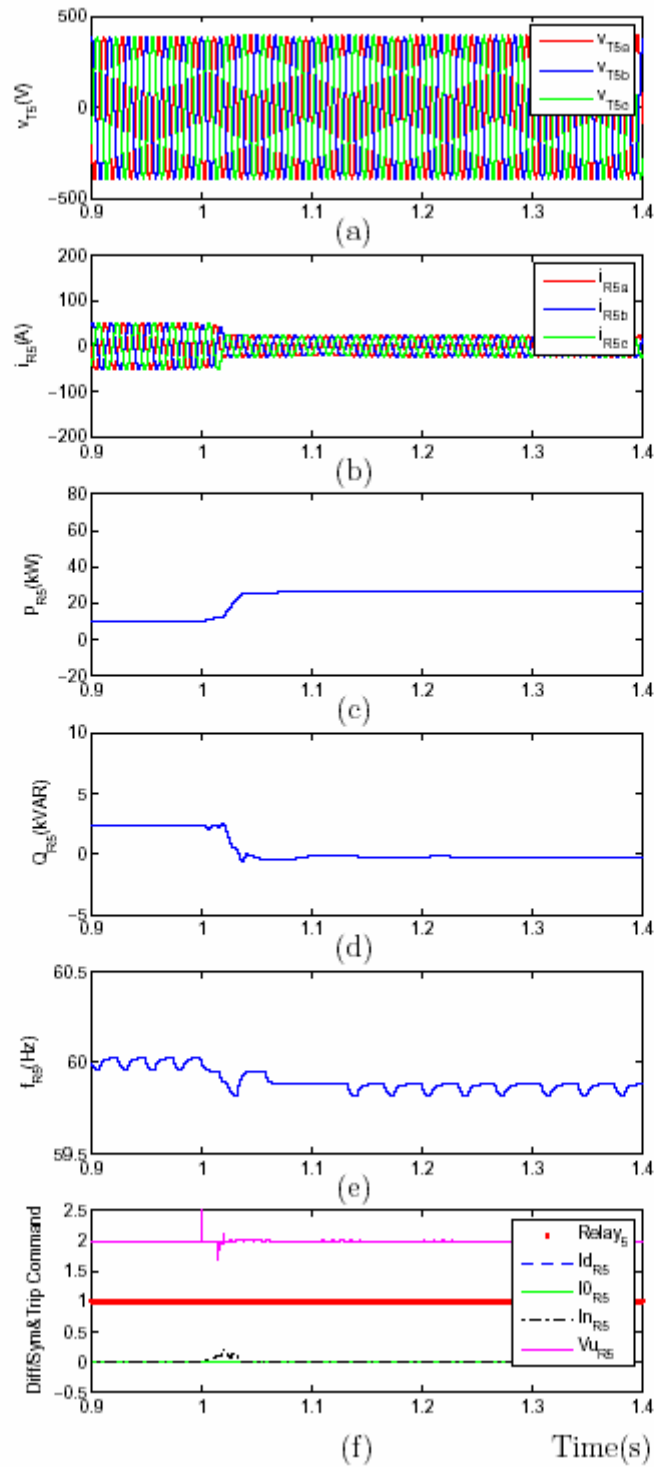
52

Figure 23: Response of the Relay 3 to a 85.5 kW LL fault in Zone 4: (a,b) three-phase voltages and currents, (c,d) real and reactive power components, (e) frequency, and (f) differential and zero- and negative-sequence current components and output command of the relay
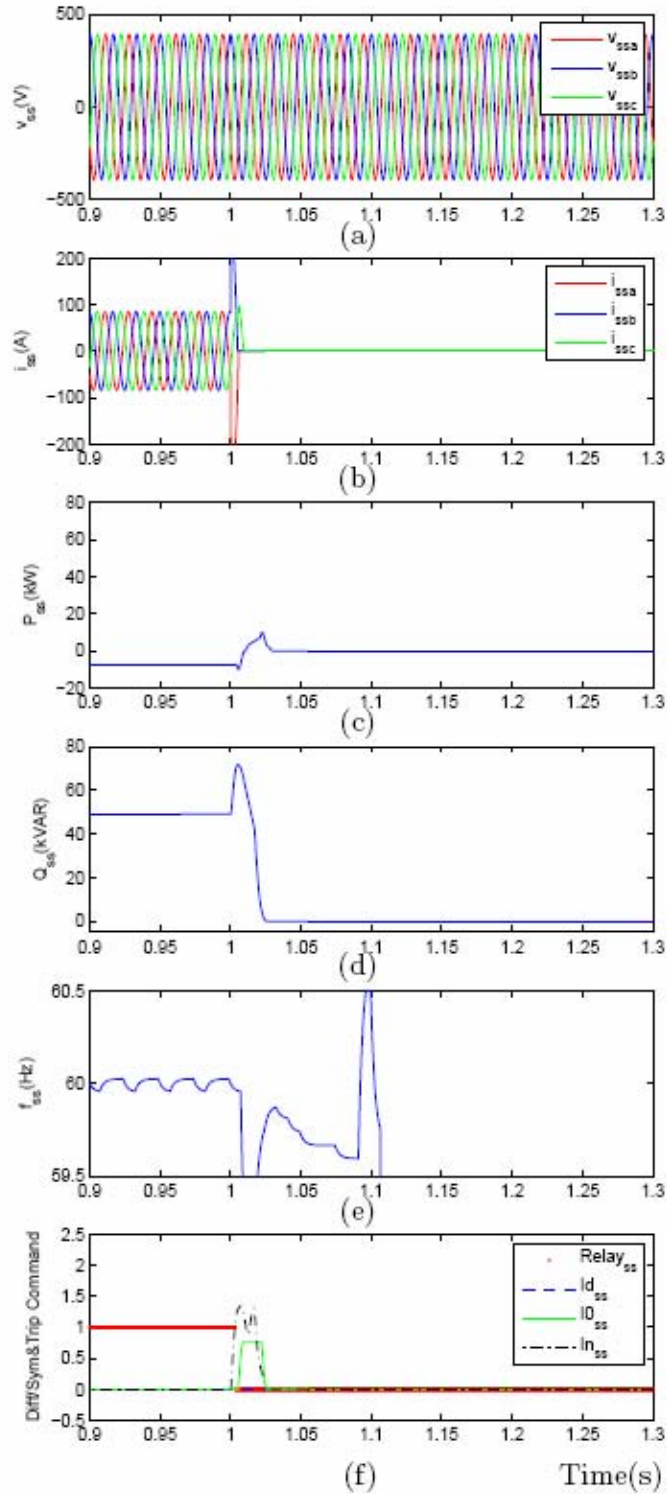
Figure 24: Response of the Relay 4 to a 85.5 kW LL fault in Zone 4: (a,b) three-phase voltages and currents, (c,d) real and reactive power components, (e) frequency, and (f) differential and zero- and negative-sequence current components and output command of the relay
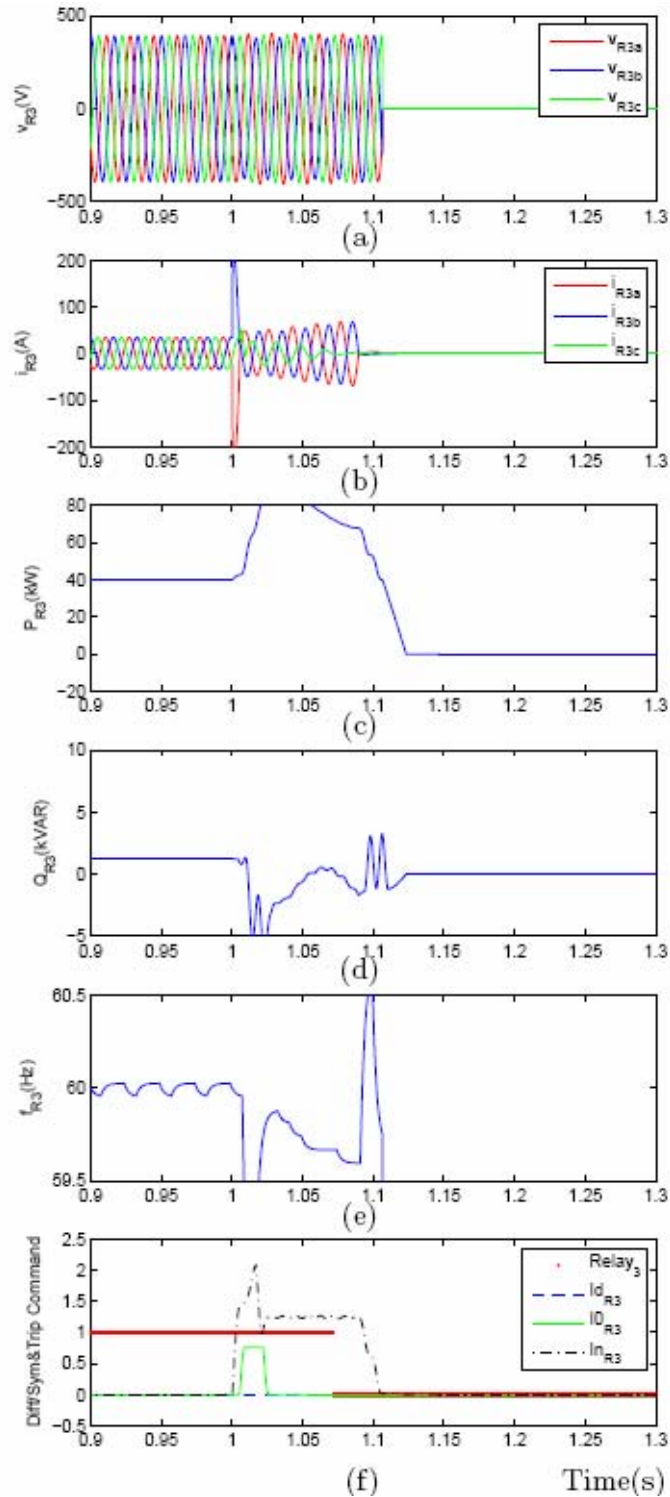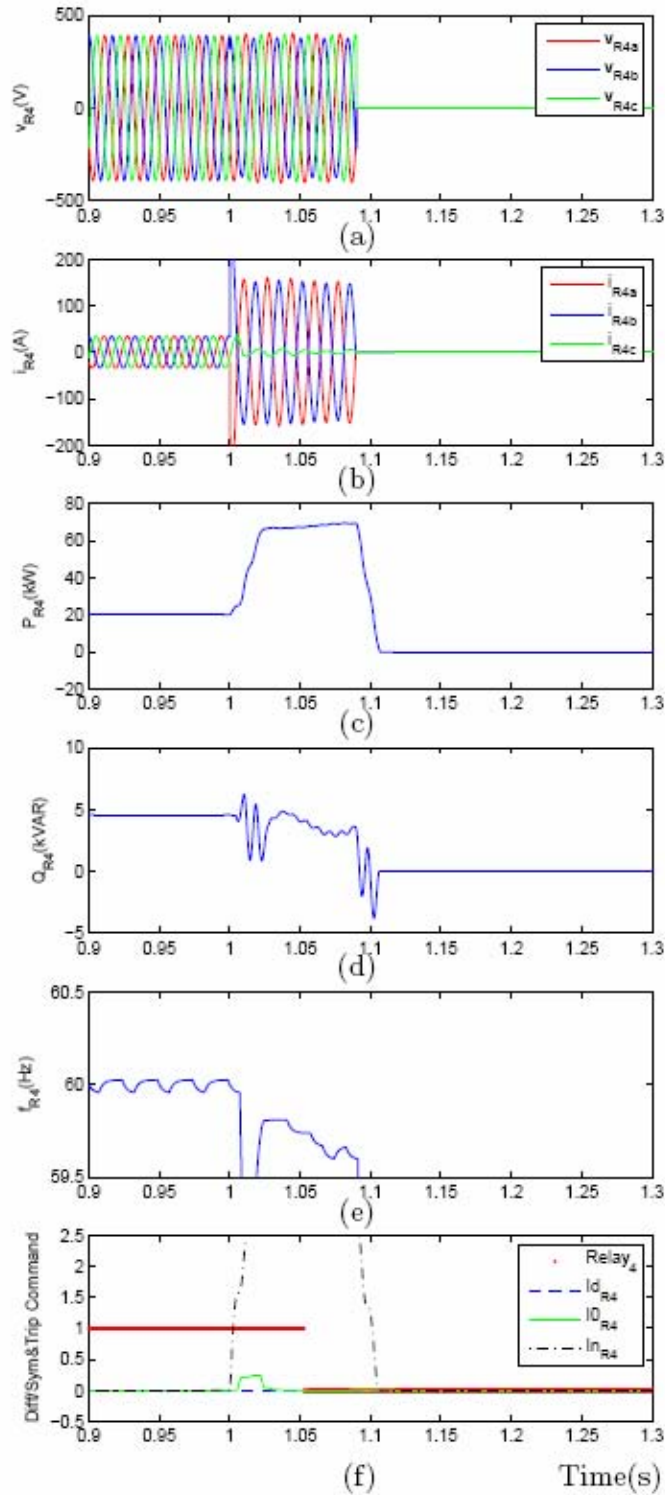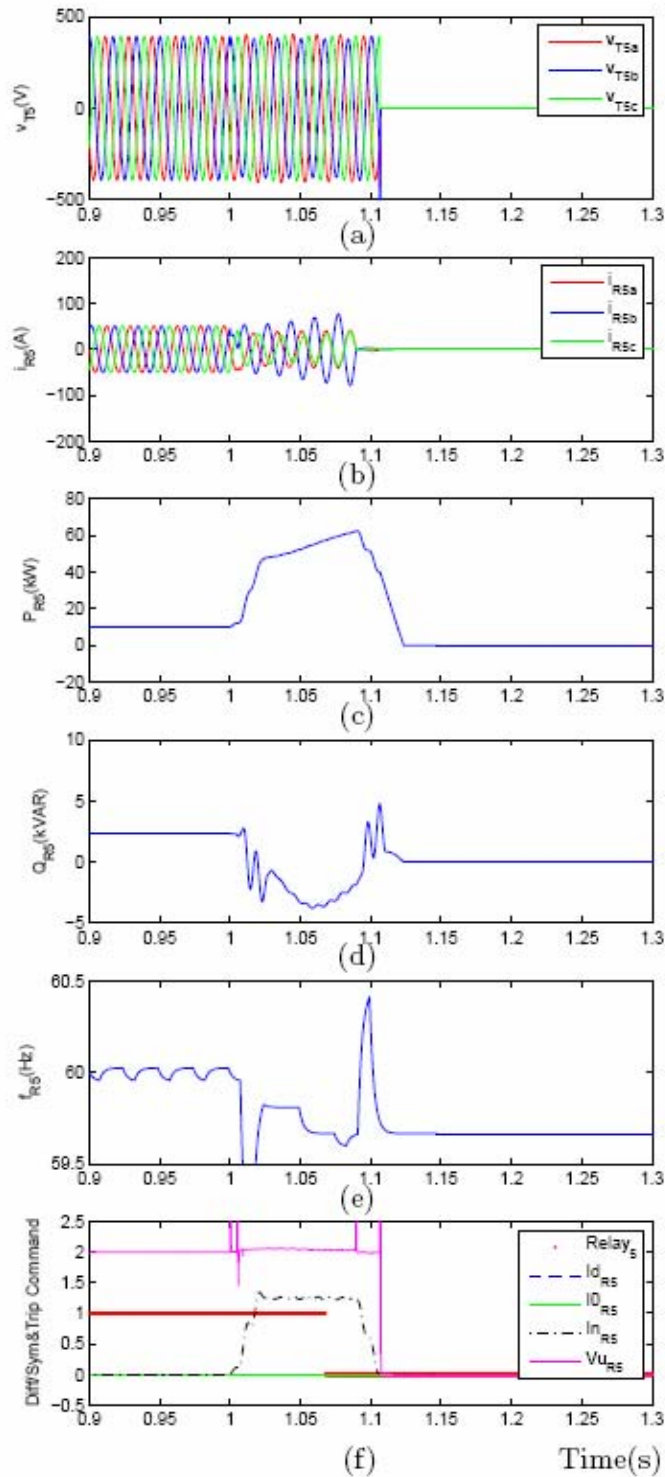
54

Figure 25: Response of the Relay 5 to a 85.5 kW LL fault in Zone 4: (a,b) three-phase voltages and currents, (c,d) real and reactive power components, (e) frequency, and (f) differential and zero- and negative-sequence current components, negative-sequence voltage component at the transformer T_{51} and output command of the relay

55

Line-to-Line Fault in Zone 3

The AEP microgrid of Fig. 1 is operating at steady-state conditions with the source and load settings as explained in Section 5 and an LL fault with a resistance of 2.695 Ohms is applied in Zone 3 at t=1.0 s. Figs. 27(a)-(e) to Figs. 20(a)-(e) show variations of the three-phase voltages and currents, the real and reactive power components, and the frequencies measured at the Relays 2, 3, 4 and 5, respectively, in response to the LL fault.

Fig. 26(f) shows that the Relay 2 commands the static switch to trip shortly after the fault when the relay detects a negative-sequence current component that exceeds 1.0 pu (95 A). Fig. 27(f) shows that the Relay 3 commands CB_{31} to trip since magnitude of the negative-sequence current component at the relay is above 1.0 pu for a period more than 50 ms (3 cycles). Fig. 28(f) shows that the Relay 4 sends a trip command to the circuit breaker CB_{41} since magnitude of the negative-sequence current component at the relay is greater than 1.0 pu for a period more than 50 ms. Fig. 29(f) shows that the Relay 5 commands CB_{51} to trip since magnitude of the negative-sequence current component at the relay is above 1.0 pu for a period more than 50 ms. Magnitudes of the differential and zero-sequence current components of all relays do not exceed the corresponding thresholds of 15 A and 35 A.

For the case of an LL fault in Zone 3, the static switch islands the microgrid and the breakers CB_{31}, CB_{41} and CB_{51} disconnects all zones of the microgrid and shut down all the microsource located inside the microgrid. The results shown in Fig. 26 to Fig. 29 demonstrate that the developed protection system is able to protect the AEP microgrid against an LL fault in Zone 3 with a power of 85.5 kW by clearing the fault and disconnecting all protection zones of the microgrid. Since the fault current increases as the fault power increases, it is concluded that the microgrid protection system is able to protect all LL faults in Zone 3 with a power more than or equal to 85.5 kW.
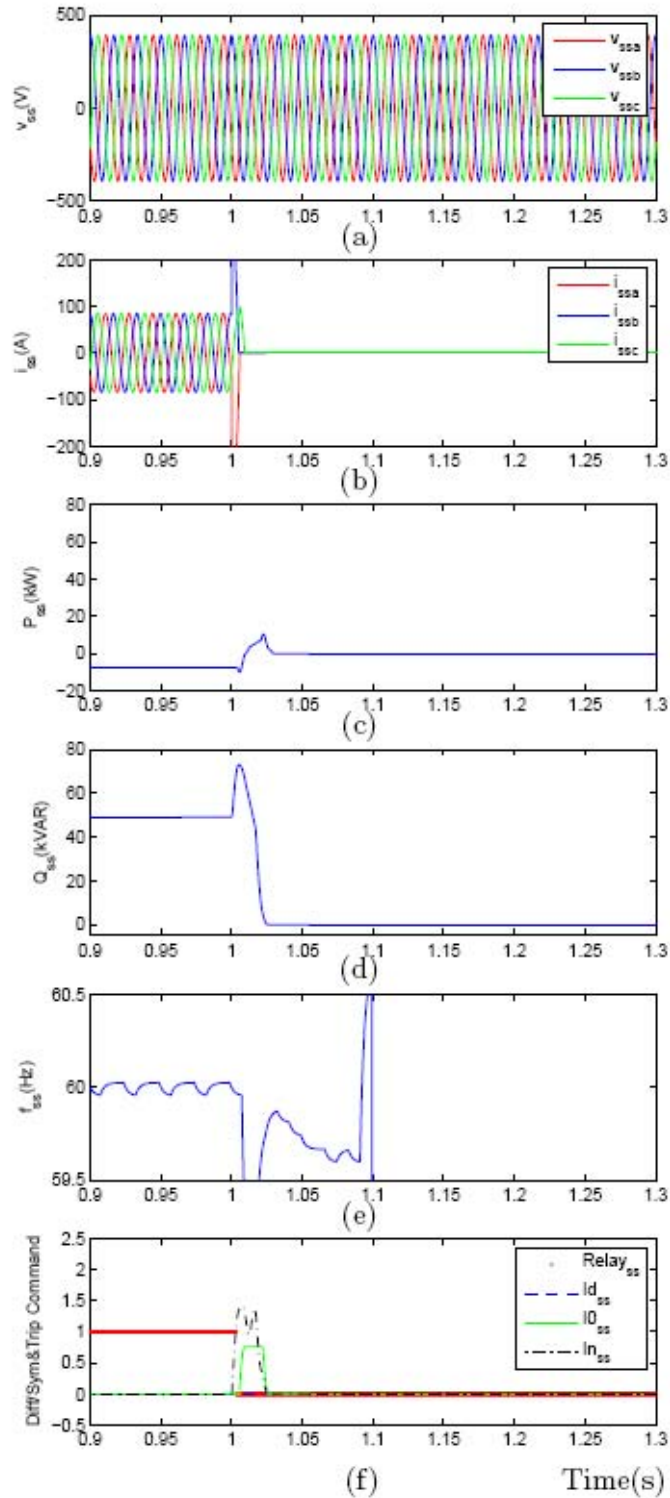
Figure 26: Response of the Relay 2 to a 85.5 kW LL fault in Zone 3: (a,b) three-phase voltages and currents, (c,d) real and reactive power components, (e) frequency, and   (f) differential and zero- and negative-sequence current components and output command of the relay

Figure 27: Response of the Relay 3 to a 85.5 kW LL fault in Zone 3: (a,b) three-phase voltages and currents, (c,d) real and reactive power components, (e) frequency, and (f) differential and zero- and negative-sequence current components and output command of the relay

Figure 28: Response of the Relay 4 to a 85.5 kW LL fault in Zone 3: (a,b) three-phase voltages and currents, (c,d) real and reactive power components, (e) frequency, and   (f) differential and zero- and negative-sequence current components and output command of the relay
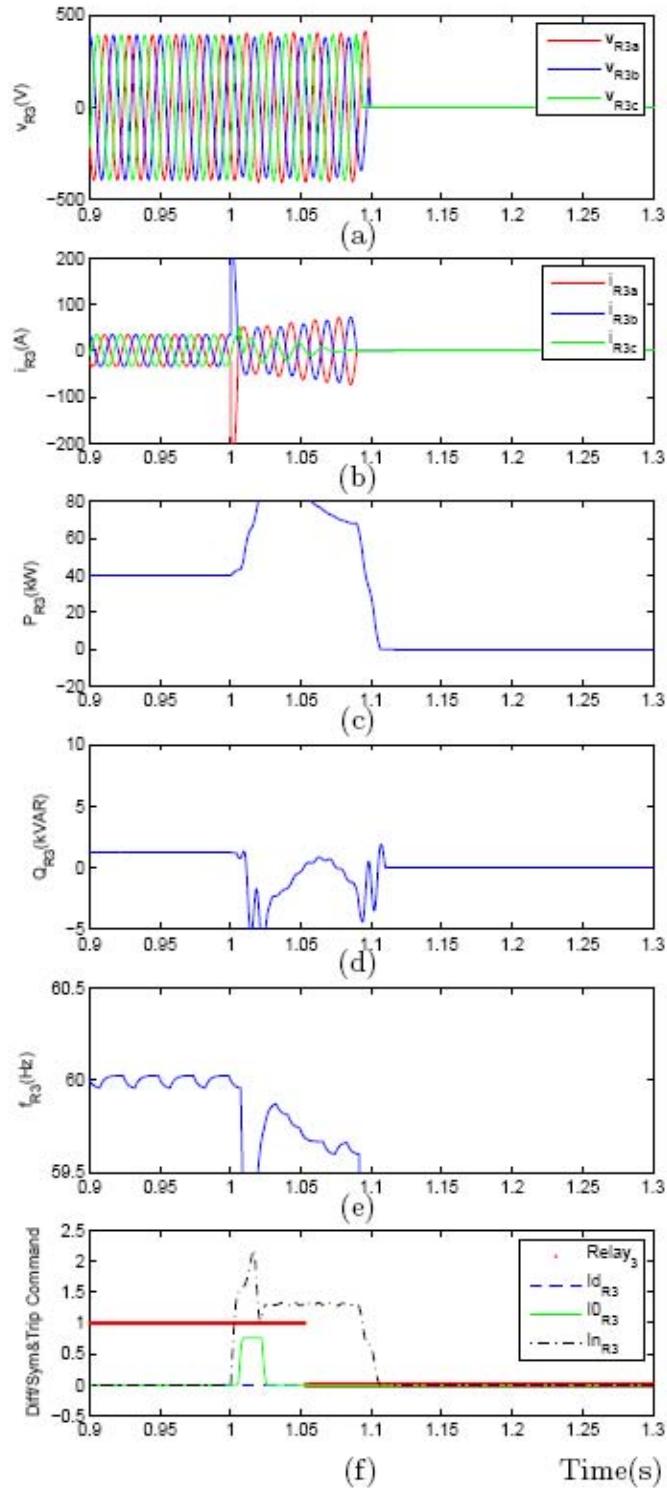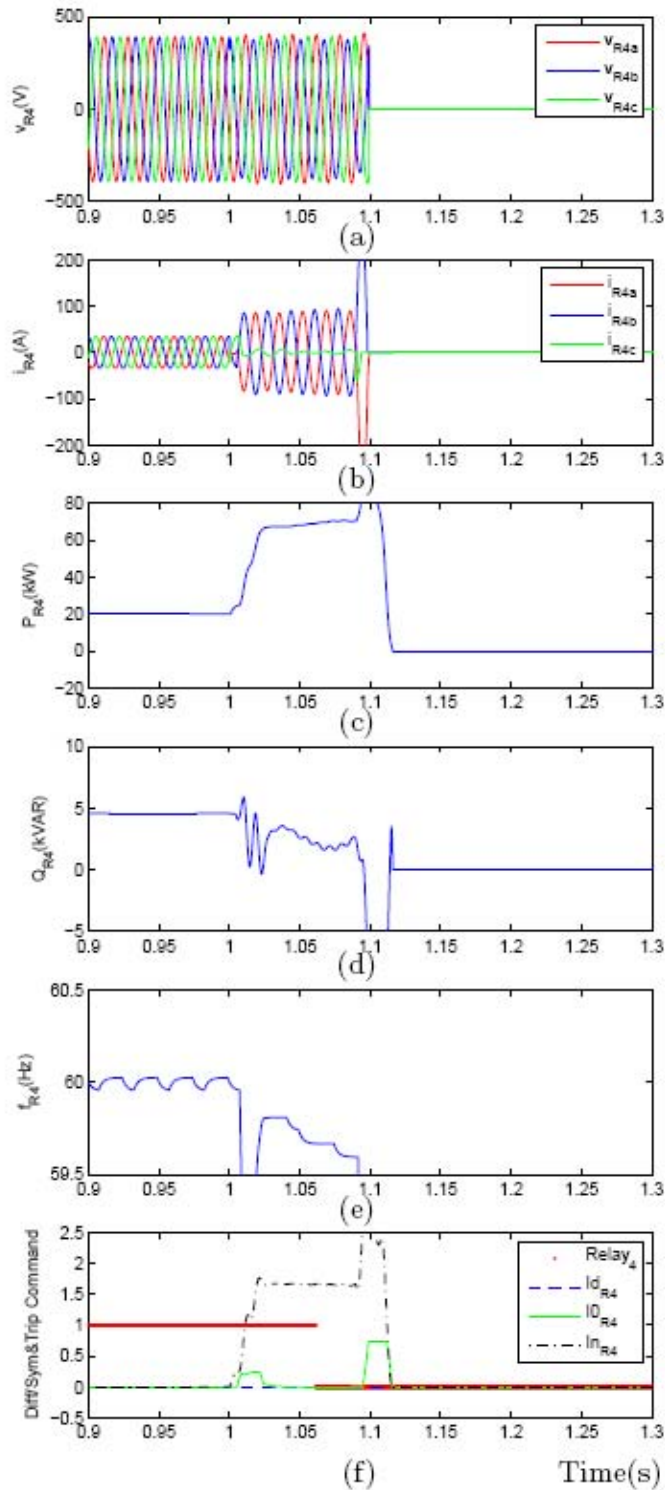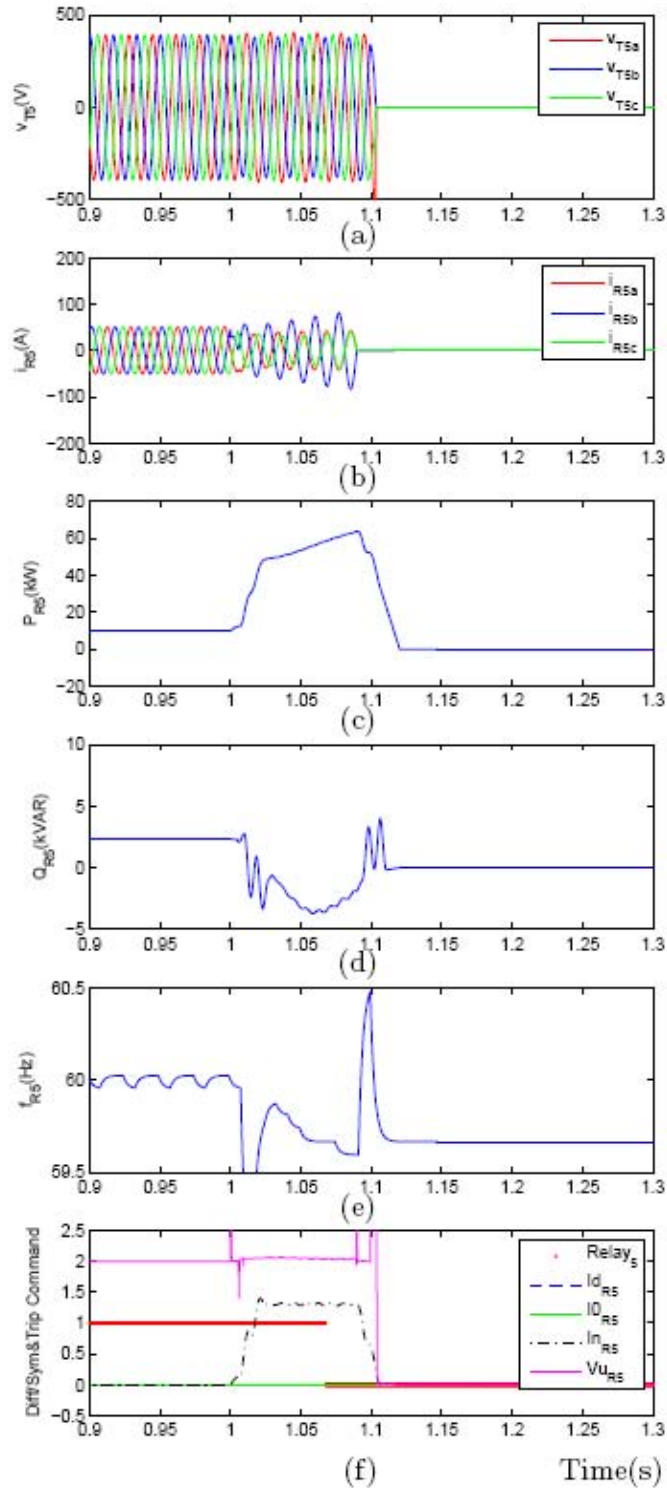
59

Figure 29: Response of the Relay 5 to a 85.5 kW LL fault in Zone 3: (a,b) three-phase voltages and currents, (c,d) real and reactive power components, (e) frequency, and (f) differential and zero- and negative-sequence current components, negative-sequence voltage component at the transformer T_{51} and output command of the relay

Line-to-Line Fault in Zone 2

The AEP microgrid of Fig. 1 is operating at steady-state conditions with the source and load settings as explained in Section 5 and an LL fault with a resistance of 2.695 Ohms is applied in Zone 2 at t=1.0 s. Figs. 31(a)-(e) to Figs. 34(a)-(e) show variations of the three-phase voltages and currents, the real and reactive power components, and the frequencies measured at the Relays 2, 3, 4 and 5, respectively, in response to the LL fault.

Fig. 30(f) shows that the Relay 2 commands the static switch to trip shortly after the fault when the relay detects a negative-sequence current component that exceeds 1.0 pu (95 A). Fig. 31(f) shows that the Relay 3 commands CB_{31} to trip since magnitude of the negative-sequence current component at the relay is above 1.0 pu for a period more than 50 ms (3 cycles). Fig. 32(f) shows that the Relay 4 sends a trip command to the circuit breaker CB_{41} since magnitude of the negative-sequence current component at the relay is greater than 1.0 pu for a period more than 50 ms. Fig. 33(f) shows that the Relay 5 commands CB_{51} to trip since magnitude of the negative-sequence current component at the relay is above 1.0 pu for a period more than 50 ms. Magnitudes of the differential and zero-sequence current components of all relays do not exceed the corresponding thresholds of 15 A and 35 A.

For the case of an LL fault in Zone 2, the static switch islands the microgrid and the breakers CB_{31}, CB_{41} and CB_{51} disconnects all zones of the microgrid and shut down all the microsource located inside the microgrid. The results shown in Fig. 30 to Fig. 33 demonstrate that the developed protection system is able to protect the AEP microgrid against an LL fault in Zone 2 with a power of 85.5 kW by clearing the fault and disconnecting all protection zones of the microgrid. Since the fault current increases as the fault power increases, it is concluded that the microgrid protection system is able to protect all LL faults in Zone 2 with a power more than or equal to 85.5 kW.
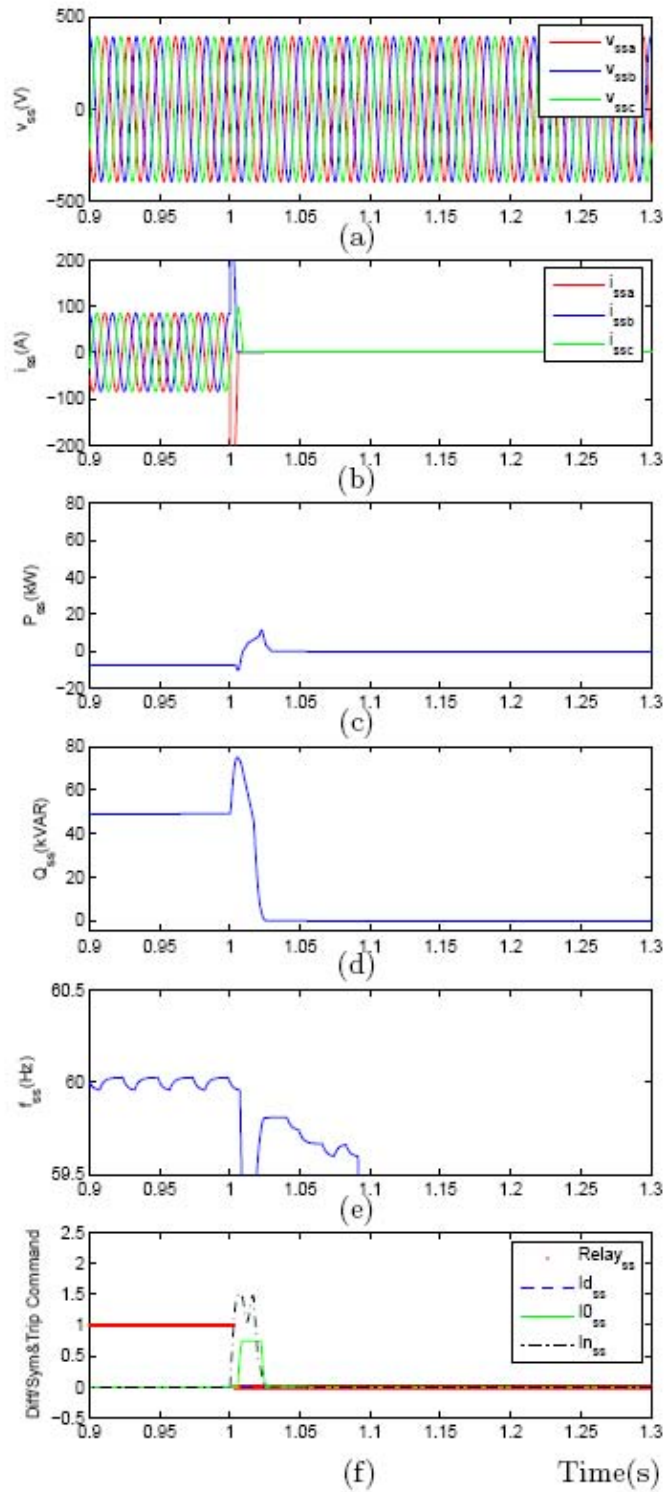
Figure 30: Response of the Relay 2 to a 85.5 kW LL fault in Zone 2: (a,b) three-phase voltages and currents, (c,d) real and reactive power components, (e) frequency, and (f) differential and zero- and negative-sequence current components and output command of the relay

Figure 31: Response of the Relay 3 to a 85.5 kW LL fault in Zone 2: (a,b) three-phase voltages and currents, (c,d) real and reactive power components, (e) frequency, and (f) differential and zero- and negative-sequence current components and output command of the relay
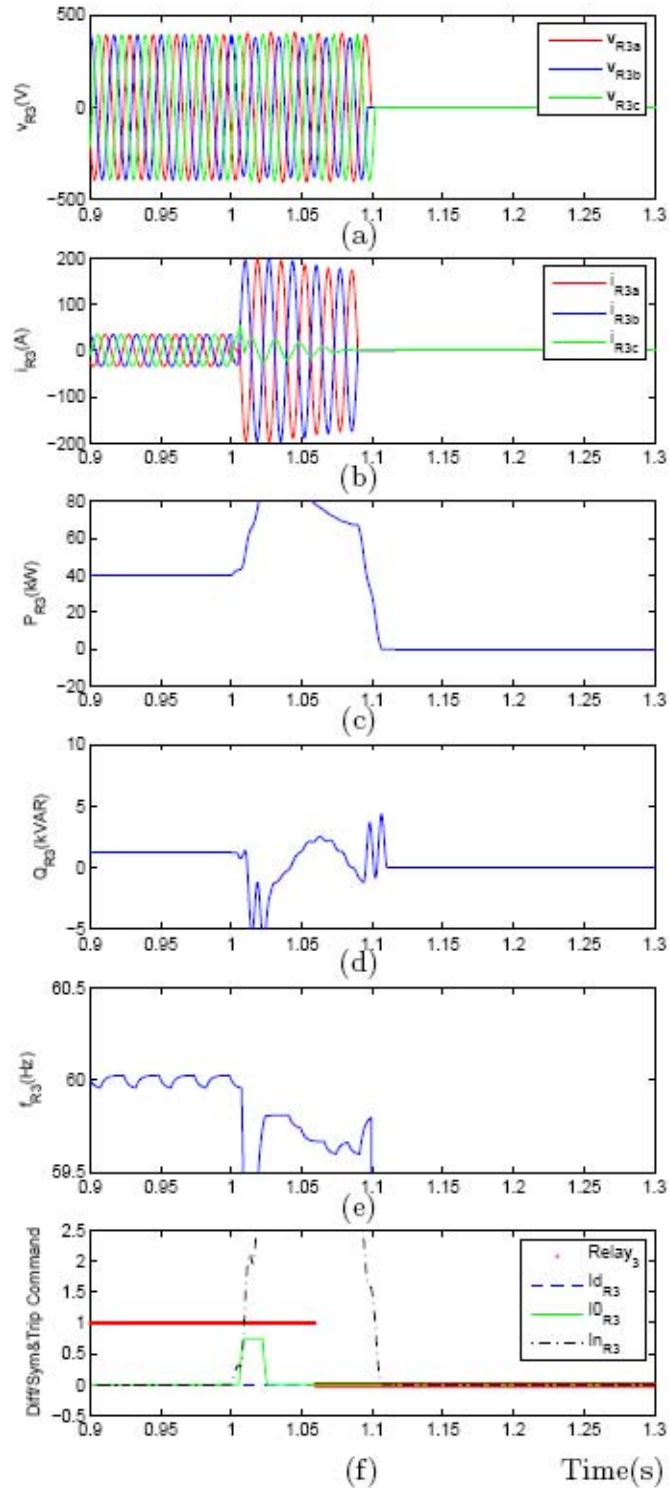
Figure 32: Response of the Relay 4 to a 85.5 kW LL fault in Zone 2: (a,b) three-phase voltages and currents, (c,d) real and reactive power components, (e) frequency, and (f) differential and zero- and negative-sequence current components and output command of the relay
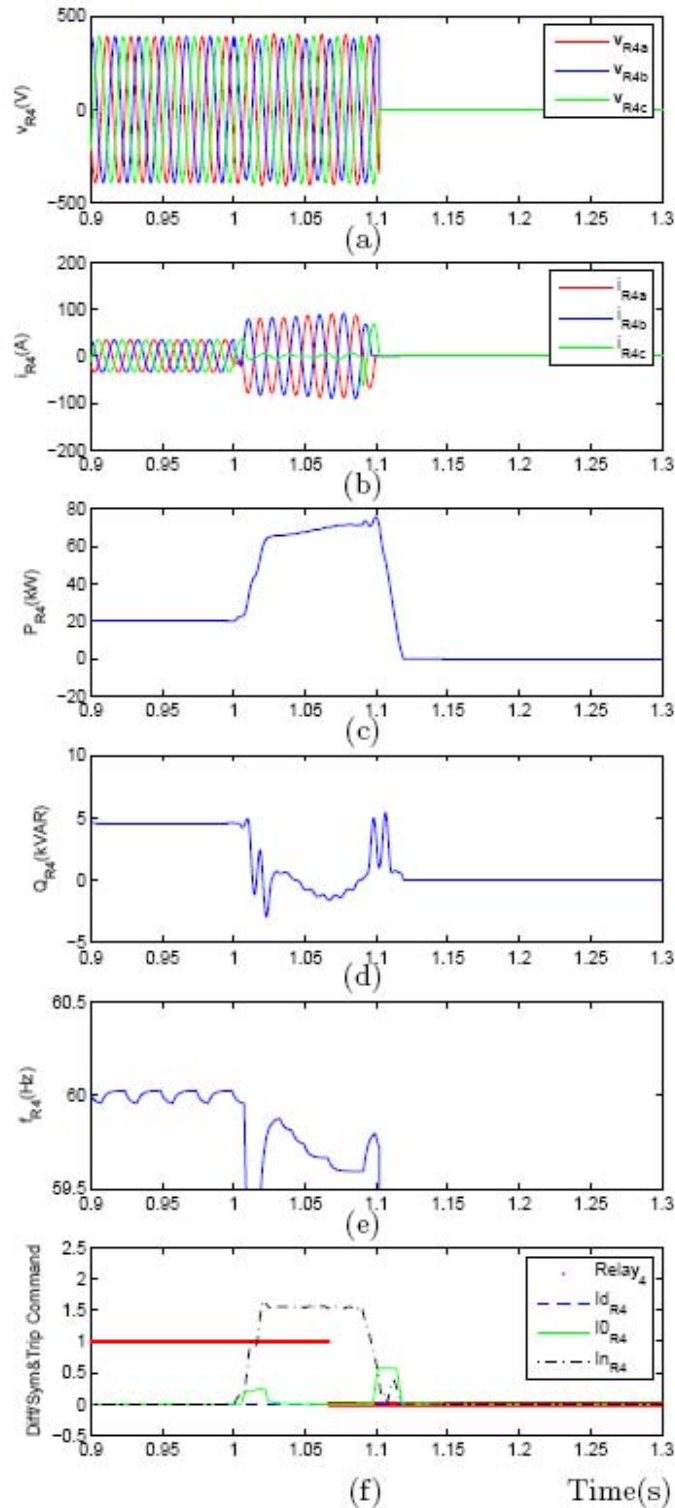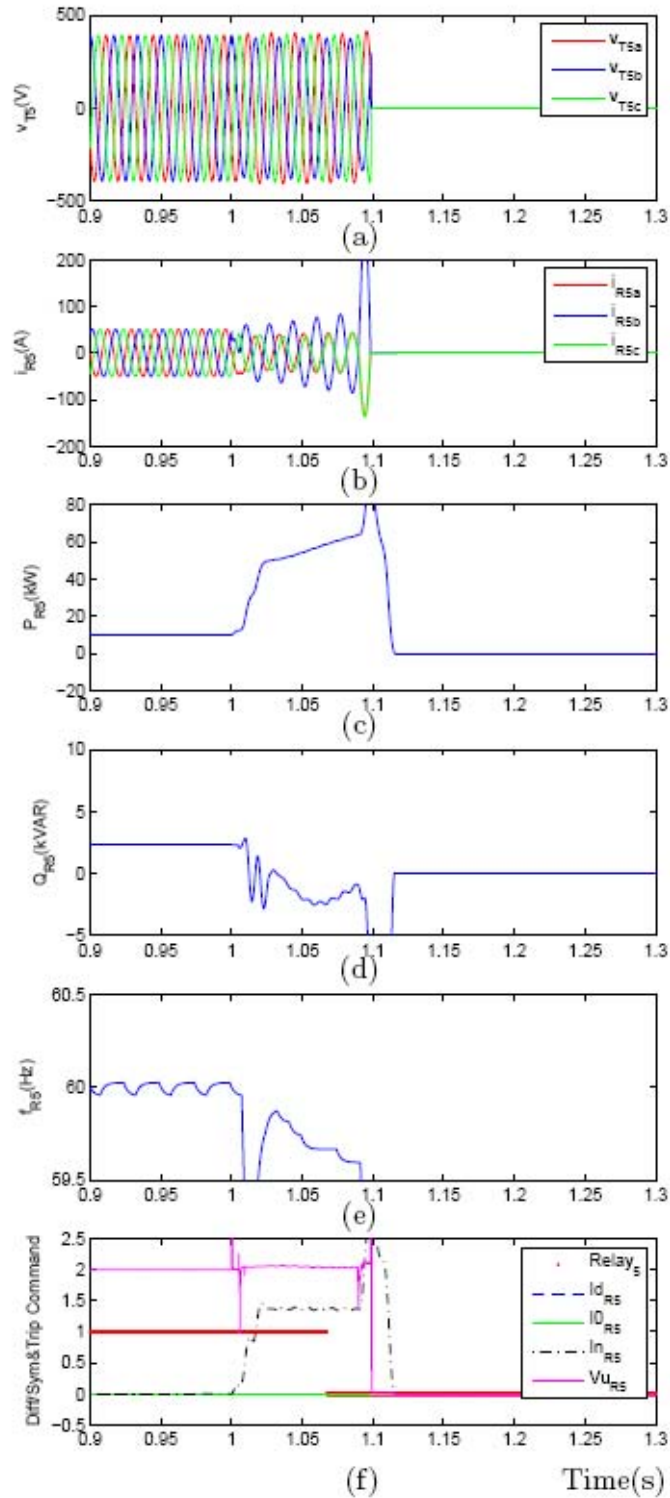
Figure 33: Response of the Relay 5 to a 85.5 kW LL fault in Zone 2: (a,b) three-phase voltages and currents, (c,d) real and reactive power components, (e) frequency, and (f) differential and zero- and negative-sequence current components, negative-sequence voltage component at the transformer T_{51} and output command of the relay

Line-to-Line Fault in Zone 5

The AEP microgrid of Fig. 1 is operating at steady-state conditions with the source and load settings as explained in Section 5 and an LL fault with a resistance of 2.695 Ohms is applied in Zone 5 at t=1.0 s. Figs. 35(a)-(e) to Figs. 38(a)-(e) show variations of the three-phase voltages and currents, the real and reactive power components, and the frequencies measured at the Relays 2, 3, 4 and 5, respectively, in response to the LL fault.

Fig. 34(f) shows that the Relay 2 commands the static switch to trip shortly after the fault when the relay detects a negative-sequence current component that exceeds 1.0 pu (95 A). Fig. 35(f) shows that the Relay 3 commands CB_{31} to trip since magnitude of the negative-sequence current component at the relay is above 1.0 pu for a period more than 50 ms (3 cycles). Fig. 36(f) shows that the Relay 4 sends a trip command to the circuit breaker CB_{41} since magnitude of the negative-sequence current component at the relay is greater than 1.0 pu for a period more than 50 ms. Fig. 37(f) shows that the Relay 5 commands CB_{51} to trip since magnitude of the negative-sequence current component at the relay is above 1.0 pu for a period more than 50 ms. Magnitudes of the differential and zero-sequence current components of all relays do not exceed the corresponding thresholds of 15 A and 35 A.

For the case of an LL fault in Zone 5, the static switch islands the microgrid and the breakers CB_{31}, CB_{41} and CB_{51} disconnects all zones of the microgrid and shut down all the microsource located inside the microgrid. The results shown in Fig. 34 to Fig. 37 demonstrate that the developed protection system is able to protect the AEP microgrid against an LL fault in Zone 5 with a power of 85.5 kW by clearing the fault and disconnecting all protection zones of the microgrid. Since the fault current increases as the fault power increases, it is concluded that the microgrid protection system is able to protect all LL faults in Zone 5 with a power more than or equal to 85.5 kW.
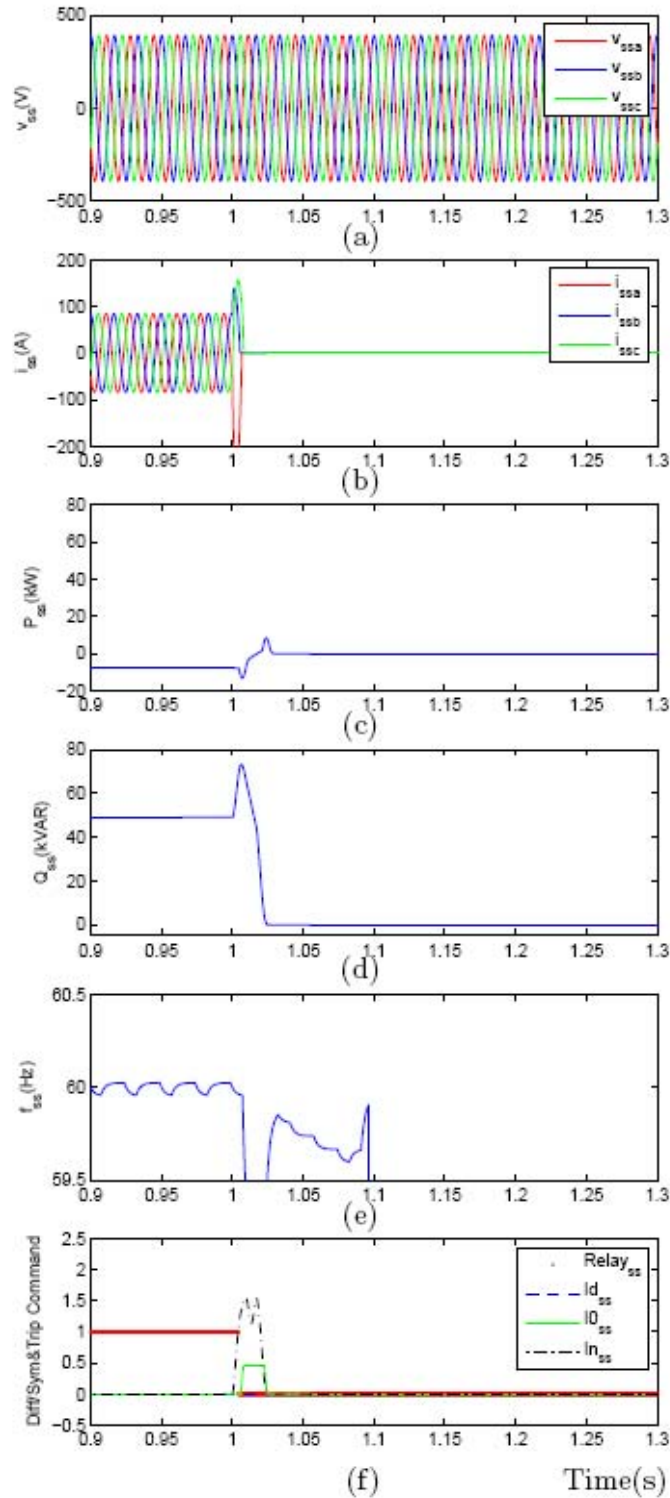
Figure 34: Response of the Relay 2 to a 85.5 kW LL fault in Zone 5: (a,b) three-phase voltages and currents, (c,d) real and reactive power components, (e) frequency, and (f) differential and zero- and negative-sequence current components and output command of the relay
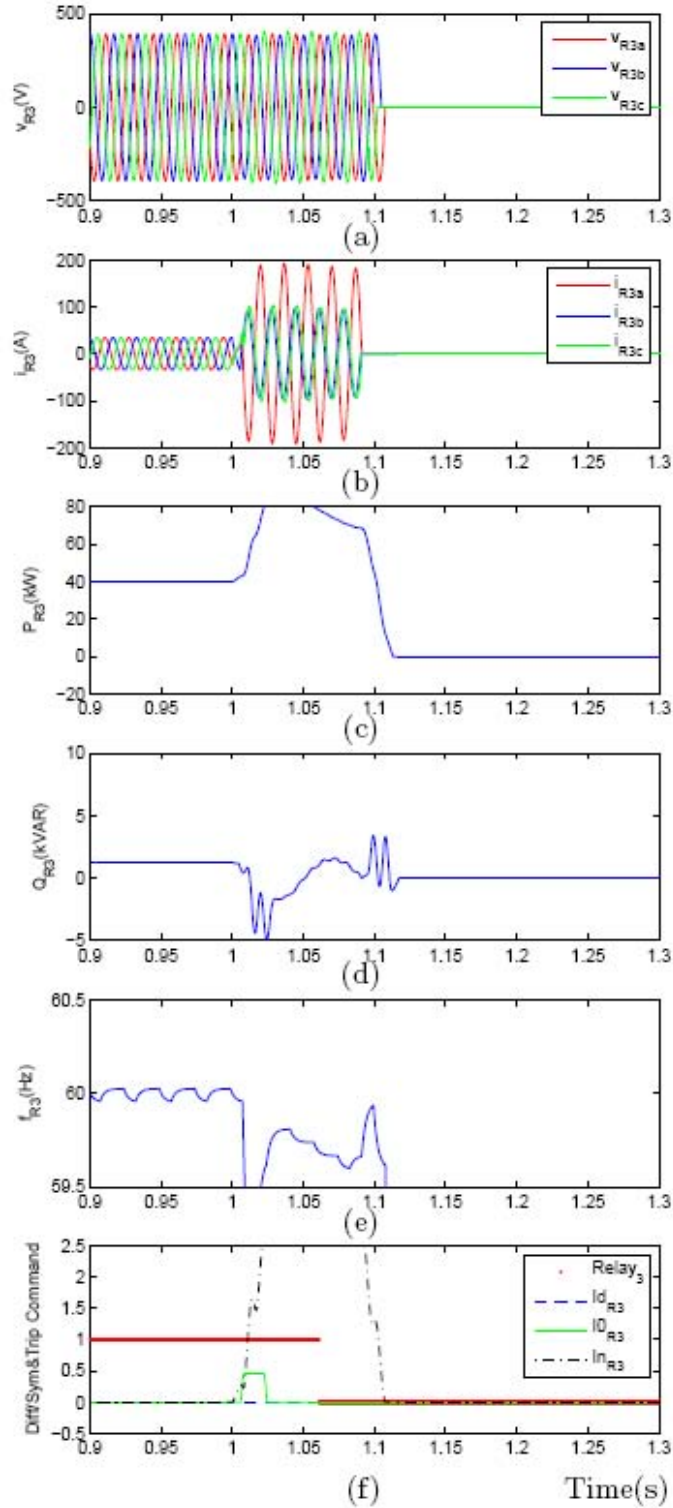
Figure 35: Response of the Relay 3 to a 85.5 kW LL fault in Zone 5: (a,b) three-phase voltages and currents, (c,d) real and reactive power components, (e) frequency, and (f) differential and zero- and negative-sequence current components and output command of the relay

Figure 36: Response of the Relay 4 to a 85.5 kW LL fault in Zone 5: (a,b) three-phase voltages and currents, (c,d) real and reactive power components, (e) frequency, and (f) differential and zero- and negative-sequence current components and output command of the relay
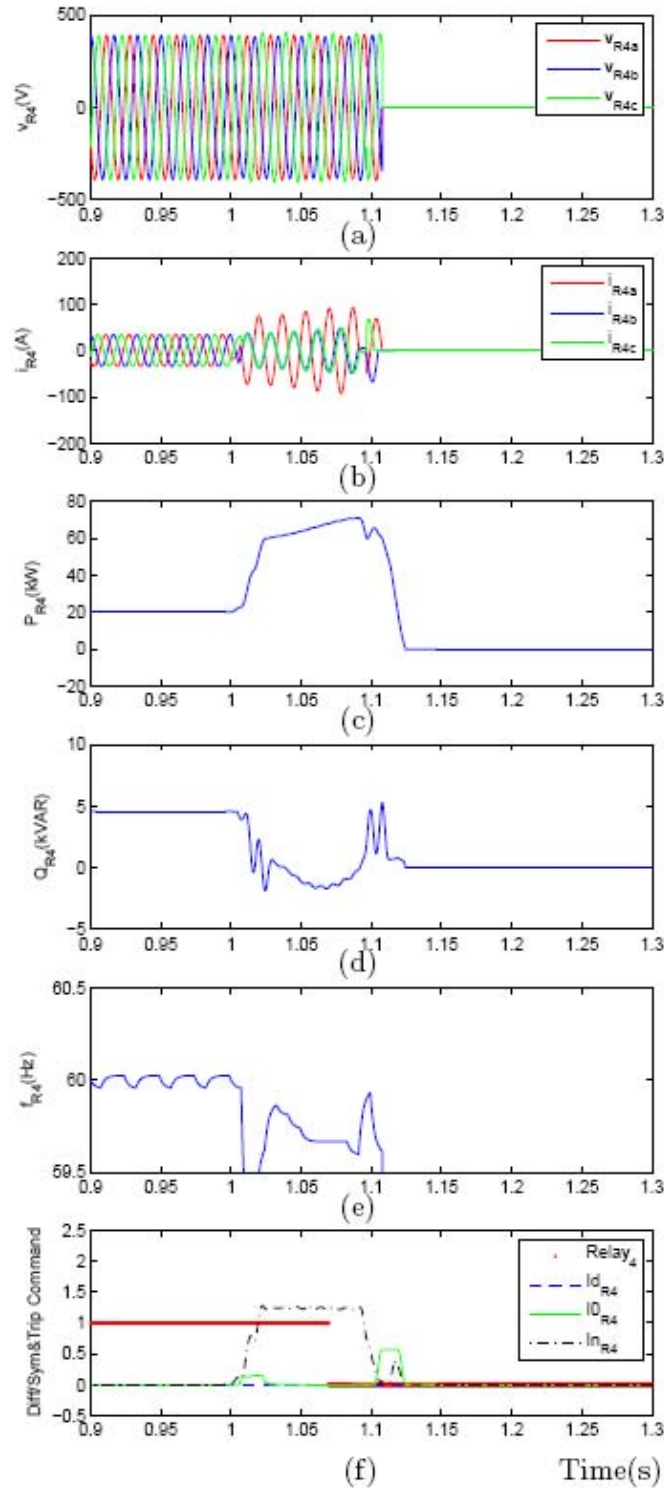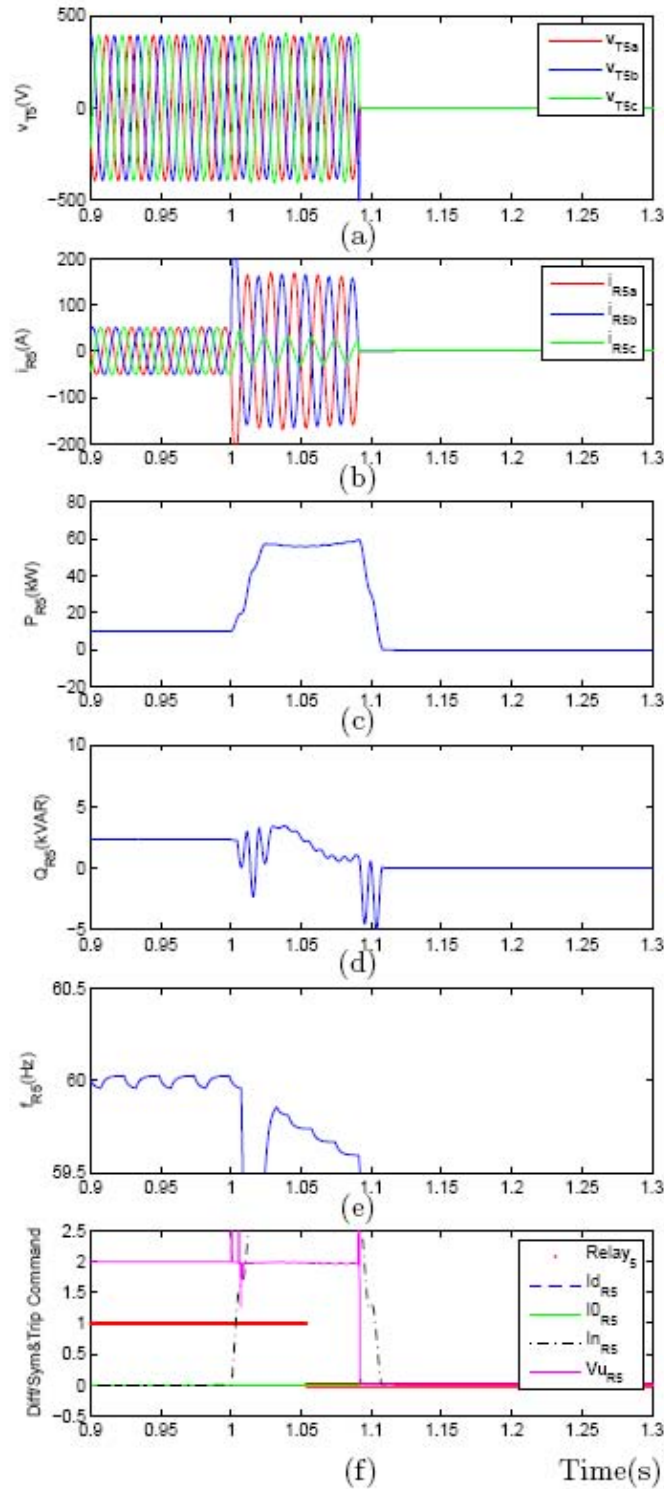
69

Figure 37: Response of the Relay 5 to a 85.5 kW LL fault in Zone 5: (a,b) three-phase voltages and currents, (c,d) real and reactive power components, (e) frequency, and (f) differential and zero- and negative-sequence current components, negative-sequence voltage component at the transformer *T*51 and output command of the relay

Line-to-Line Fault in Zone 6

The AEP microgrid of Fig. 1 is operating at steady-state conditions with the source and load settings as explained in Section 5 and an LL fault with a resistance of 2.695 Ohms is applied in Zone 6 at t=1.0 s. Figs. 39(a)-(e) to Figs. 42(a)-(e) show variations of the three-phase voltages and currents, the real and reactive power components, and the frequencies measured at the Relays 2, 3, 4 and 5, respectively, in response to the LL fault.

Fig. 38(f) shows that the Relay 2 commands the static switch to trip shortly after the fault when the relay detects a negative-sequence current component that exceeds 1.0 pu (95 A). Fig. 39(f) shows that the Relay 3 does not command for a trip since none of its fault detection parameters, i.e. the differential and symmetrical current components, exceeds the threshold of 1.0 pu. Fig. 40(f) shows that the Relay 4 does not command for a trip since none of its fault detection parameters, i.e. the differential and symmetrical current components, exceeds the threshold of 1.0 pu. Fig. 41(f) shows that the Relay 5 does not command for a trip since none of its fault detection parameters, i.e. the differential and symmetrical current components, exceeds the threshold of 1.0 pu.

For the case of an LL fault in Zone 6, the static switch islands the microgrid. The Zones 2, 3, 4 and 5 of the microgrid and the microsources A_1, A_2 and B_1 continue the operation subsequent to the fault detection and its clearance. The results shown in Fig. 38 to Fig. 41 demonstrate that the developed protection system is able to protect the AEP microgrid against an LL fault in Zone 6 with a power of 85.5 kW by disconnecting the static switch. Since the fault current increases as the fault power increases, it is concluded that the microgrid protection system is able to protect all LL faults in Zone 6 with a power more than or equal to 85.5 kW.
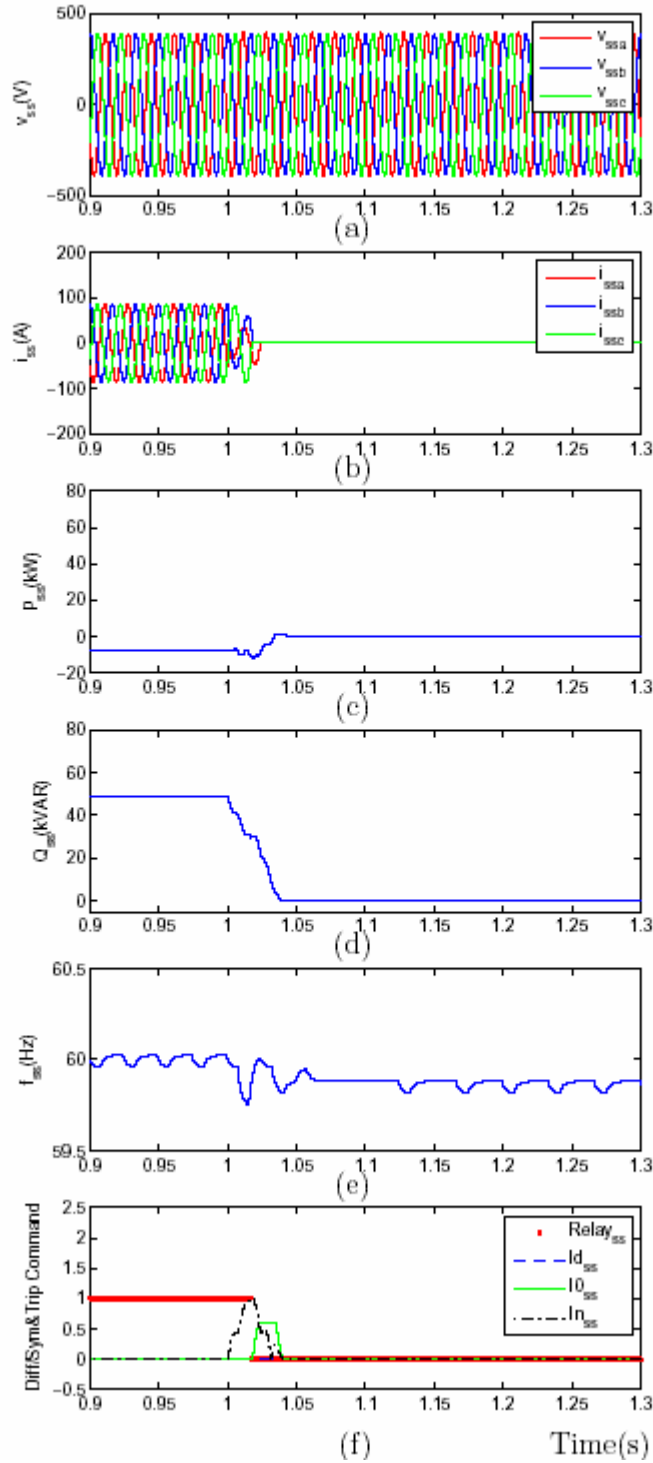
Figure 38: Response of the Relay 2 to a 85.5 kW LL fault in Zone 6: (a,b) three-phase voltages and currents, (c,d) real and reactive power components, (e) frequency, and (f) differential and zero- and negative-sequence current components and output command of the relay
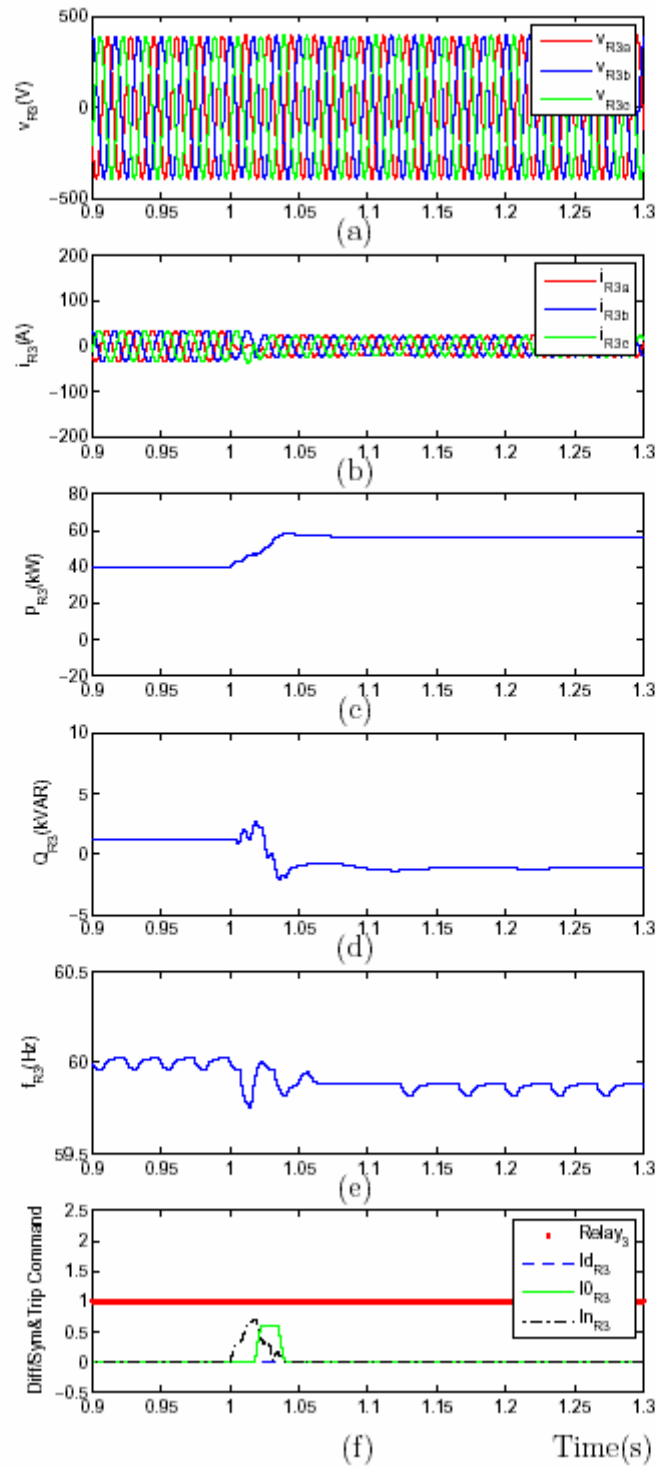
72

Figure 39: Response of the Relay 3 to a 85.5 kW LL fault in Zone 6: (a,b) three-phase voltages and currents, (c,d) real and reactive power components, (e) frequency, and (f) differential and zero- and negative-sequence current components and output command of the relay
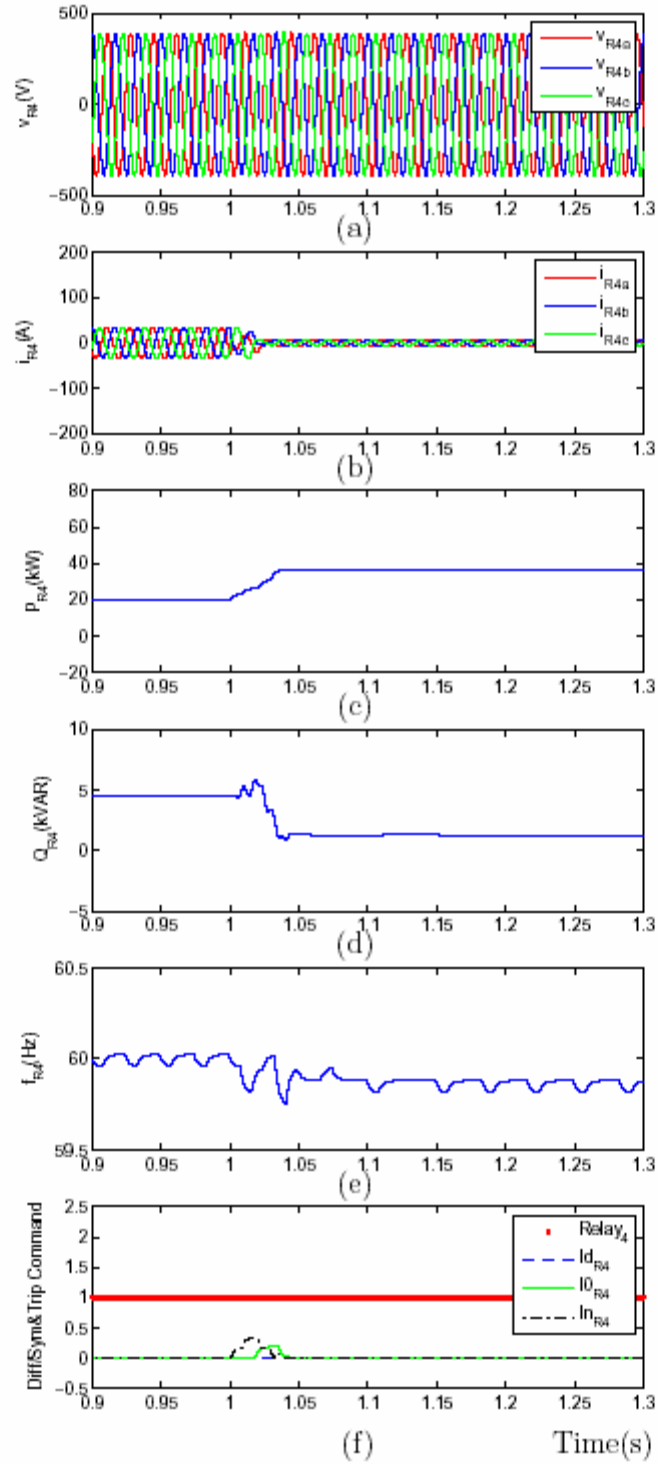
Figure 40: Response of the Relay 4 to a 85.5 kW LL fault in Zone 6: (a,b) three-phase voltages and currents, (c,d) real and reactive power components, (e) frequency, and (f) differential and zero- and negative-sequence current components and output command of the relay
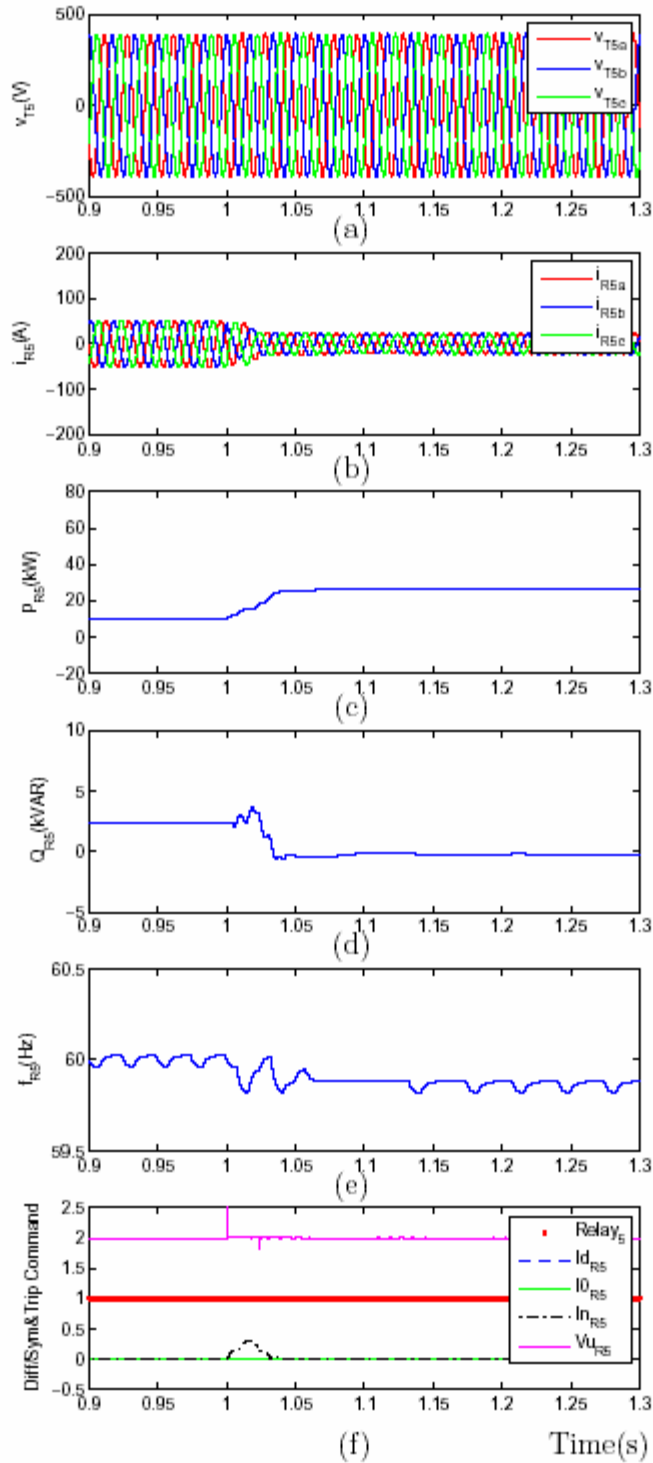
Figure 41: Response of the Relay 5 to a 85.5 kW LL fault in Zone 6: (a,b) three-phase voltages and currents, (c,d) real and reactive power components, (e) frequency, and (f) differential and zero- and negative-sequence current components, negative-sequence voltage component at the transformer *T*51 and output command of the relay

Bibliography

[1] P. Piagi, "Microgrid control," Ph.D. dissertation, University of Wisconsin-Madison, 2005

[2] R. H. Lasseter and P. Piagi, "Control and design of microgrid components," *PSERC Publication 06-03,* University of Wisconsin-Madison, January 2006

[3] H. Nikkhajoei, P. Piagi, and R. H. Lasseter, "EMTP Simulation of Single Line to Ground Fault in Zone 3 of AEP Microgrid System," Wisconsin Power Electronics Research Center, University of Wisconsin-Madison, August 2006

[4] A. R. Bergen, "Power Systems Analysis", *Prentice-Hall Publications*, 1986

[5] "CERTS Test Bed Protection Device Selection and Settings," Northern Power Systems Energy Technology Laboratory, 2005

[6] B. Fleming, "Creating a Phase Current Unbalance Alarm/Supervision Function in the SEL-351 Relay," Schweitzer Engineering Laboratories, Inc., 1998

[7] F. Calero, "Rebirth of negative-Sequence Quantities in protective Relaying with microprocessor-Based relays," Schweitzer Engineering Laboratories, Inc., 2003

[8] A. F. Elneweihi, E. O. Scweitzer, and M. W. Feltis, "Negative-Sequence Overcurrent Element Application and Coordination in distribution Protection," *IEEE Trans. On Power Delivery*, Vol. 8, No. 3, pp. 915-924, July 1993